Kaunas University of Technology

Faculty of Mechanical Engineering and Design

Investigation of Electrical Properties of 3D Printed Carbon Fiber Reinforced Composite Structures

Master's Final Degree Project

Laurynas Bakas

Project author

Assoc. Prof. Marius Rimašauskas

Supervisor

Kaunas, 2023

Kaunas University of Technology

Faculty of Mechanical Engineering and Design

Investigation of Electrical Properties of 3D Printed Carbon Fiber Reinforced Composite Structures

Master's Final Degree Project

Mechatronics (6211EX017)

Laurynas Bakas

Project author

Assoc. Prof. Marius Rimašauskas

Supervisor

Researcher Valdas Grigaliūnas

Reviewer

Kaunas, 2023

Kaunas University of Technology

Faculty of Mechanical Engineering and Design

Laurynas Bakas

Investigation of Electrical Properties of 3D Printed Carbon Fiber Reinforced Composite Structures

Declaration of Academic Integrity

I confirm the following:

1. I have prepared the final degree project independently and honestly without any violations of the copyrights or other rights of others, following the provisions of the Law on Copyrights and Related Rights of the Republic of Lithuania, the Regulations on the Management and Transfer of Intellectual Property of Kaunas University of Technology (hereinafter – University) and the ethical requirements stipulated by the Code of Academic Ethics of the University;

2. All the data and research results provided in the final degree project are correct and obtained legally; none of the parts of this project are plagiarised from any printed or electronic sources; all the quotations and references provided in the text of the final degree project are indicated in the list of references;

3. I have not paid anyone any monetary funds for the final degree project or the parts thereof unless required by the law;

4. I understand that in the case of any discovery of the fact of dishonesty or violation of any rights of others, the academic penalties will be imposed on me under the procedure applied at the University; I will be expelled from the University and my final degree project can be submitted to the Office of the Ombudsperson for Academic Ethics and Procedures in the examination of a possible violation of academic ethics.

Laurynas Bakas

Confirmed electronically

Kaunas University of Technology

Faculty of Mechanical Engineering and Design

Task of the Master's Final Degree Project

Given to the student – Laurynas Bakas

1. Title of the Project

Investigation of Electrical Properties of 3D Printed Carbon Fiber Reinforced Composite Structures

(In English)

Anglies pluoštu sustiprintų 3D spausdintų kompozitinių struktūrų elektrinių savybių tyrimas

(In Lithuanian)

2. Aim and Tasks of the Project

Aim: to investigate the electrical resistance of 3D printed continuous carbons fiber reinforced composite structures.

Tasks:

1. to produce unidirectional 0° and 0°-90° composite structures with various carbon fiber content;
2. to test electrical resistance of composite structures under static loading;
3. to test electrical resistance of composite structures under dynamic loading;
4. to evaluate correlation between carbon fiber content and electrical resistance measured;
5. to evaluate economic benefits of 3D printed carbon fiber reinforced composite sensors.

3. Main Requirements and Conditions

Continuous carbon fiber reinforced 3D printed test specimens fabricated. Static and dynamic loading tests to be performed and resistance values measured and analyzed.

4. Additional Requirements for the Project, Report and its Annexes

Not applicable

Project author	Laurynas Bakas		2023 03 05
	(Name, Surname)	*(Signature)*	*(Date)*
Supervisor	Marius Rimašauskas		2023 03 05
	(Name, Surname)	*(Signature)*	*(Date)*
Head of study field programs	Regita Bendikienė		2023 03 05
	(Name, Surname)	*(Signature)*	*(Date)*

Bakas Laurynas. Investigation of Electrical Properties of 3D Printed Carbon Fiber Reinforced Composite Structures. Master's Final Degree Project, supervisor Assoc. Prof. Marius Rimašauskas; Faculty of Mechanical Engineering and Design, Kaunas University of Technology.

Study field and area (study field group): Production and Manufacturing Engineering (E10), Engineering Sciences (E).

Keywords: 3D printing; carbon fiber; piezo resistivity; sensor; cyclical loading.

Kaunas, 2023. 57 p.

Summary

In recent years, 3D printed continuous carbon fiber reinforced composite materials gained popularity in multiple industries mainly due to their mechanical properties. These composites provide reduced weight while keeping the same strength when compared to metals is greatly desirable in aerospace, automotive, biomedical, sports, and other industries. In addition to their mechanical properties continuous carbon fiber reinforced composites have numerous advantages, for instance, electrical properties, anti-corrosive properties and environmental impact reduction during manufacturing. Recent advancements in 3D printing technology allow to manufacture CCFRP structures rapidly with minimal wasted materials and with excellent mechanical and electrical characteristics. CCFRP composite electrical properties, such as, piezo resistivity can be beneficial in numerous applications from fatigue monitoring to structure health evaluation and load sensing. Previous research on 3D printed CCFRP composites and testing methodologies are analyzed. Testing methodology for resistance measurement during cyclical dynamic loading, as well as, static loading is developed. Piezo resistive properties of 3D printed CCFRP composites are evaluated in this project. The aim of this project is to investigate the electrical resistance of 3D printed continuous carbons fiber reinforced composite structures. There are multiple tasks to achieve the aim identified: (1) to produce unidirectional 0° and 0°-90° composite structures with various carbon fiber content; (2) to test electrical resistance of composite structures under static loading; (3) to test electrical resistance of composite structures under dynamic loading; (4) to evaluate correlation between carbon fiber content and electrical resistance measured; (5) to evaluate economic benefits of 3D printed carbon fiber reinforced composite sensors. Test specimens are 3D printed and processed for resistance measurement. Testing results are analyzed and suggestions are given. Economic benefits of 3D printing CCFRP sensors are analyzed. Conclusions drawn for static and dynamic loading of the test specimens. The findings of this project suggest that 3D printed CCFRP composites are suitable to be used as load sensors in various applications and may offer safety and space saving benefits.

Bakas Laurynas. Anglies pluoštu sustiprintų 3D spausdintų kompozitinių struktūrų elektrinių savybių tyrimas. Magistro baigiamasis projektas, vadovas doc. Marius Rimašauskas; Kauno technologijos universitetas, Mechanikos inžinerijos ir dizaino fakultetas.

Studijų kryptis ir sritis (studijų krypčių grupė): Gamybos inžinerija (E10), Inžinerijos mokslai (E).

Reikšminiai žodžiai: 3D spausdinimas; anglies pluoštas; pjezo varža; jutiklis; ciklinė apkrova.

Kaunas, 2023. 57 p.

Santrauka

Pastaraisiais metais 3D spausdinti ištęstiniu anglies pluoštu sustiprintų kompozitinių (CCFRP) medžiagų populiarumas išaugo daugelyje pramonės šakų, ypač dėl jų mechaninių savybių. Šie kompozitai sumažina detalių masę, išlaikydami tą patį atsparumą mechaninėms apkrovoms, lyginant su metalais, kas yra privalumas aviacijos, aeronautikos, automobilių, biomedicinos, sporto ir kitose pramonės šakose. Be mechaninių savybių ištęstiniu anglies pluoštu sustiprintos kompozitinės medžiagos turi ir daugybę kitų privalumų, pvz., elektrines savybes, antikorozines savybes bei sumažintą poveikį aplinkai gamybos metu. Naujausi 3D spausdinimo technologijų patobulinimai leidžia sparčiai gaminti ištęstiniu anglies pluoštu sustiprintas kompozitines struktūras su puikiomis mechaninėmis ir elektrinėmis savybėmis, taip pat, su mažesniu atliekų kiekiu. CCFRP kompozitinių medžiagų elektrinės savybės, pvz., pjezo varžumas, gali būti naudingos daugelyje pramonės šakų ir pritaikymų, nuo detales nusidėvėjimo stebėjimo iki struktūros tinkamumo naudoti vertinimo ir apkrovų jutimo. Atlikta anksčiau pateiktų 3D spausdintų CCFRP medžiagų tyrimų analizė ir išanalizuota bandymų metodologija. Sukurta bandymų metodologija elektrinei varžai matuoti statinės ir ciklinės dinaminės apkrovos metu. Šiame projekte analizuojamos 3D spausdintų struktūrų pjezo varžumo savybės. Šio projekto tikslas yra ištirti 3D spausdintų ištęstiniu anglies pluoštu sustiprintų kompozitinių struktūrų elektrinę varžą. Nustatyti keli uždaviniai, kad būtų įgyvendintas projekto tikslas: (1) pagaminti vienos krypties 0° ir 0°-90° pluošto orientacijos kompozitines struktūras su įvairiomis anglies pluošto proporcijomis, (2) ištirti kompozitinių struktūrų elektrinę varžą statinės apkrovos metu, (3) ištirti kompozitinių struktūrų elektrinę varžą dinaminės apkrovos metu, (4) įvertinti koreliaciją tarp anglies pluošto kiekio bandinyje ir išmatuotos elektrinės varžos, (5) įvertinti 3D spausdintų anglies pluoštu sustiprintų jutiklių ekonominę naudą. Bandiniai yra atspausdinti 3D spausdintuvu ir paruošti elektros varžos matavimui. Bandymų rezultatai yra analizuojami ir pateikiamos rekomendacijos. Taip pat analizuojami CCFRP jutiklių ekonominiai pranašumai. Šio projekto išvados rodo, kad 3D spausdinti anglies pluoštu sustiprinti kompozitai yra tinkami naudoti kaip apkrovos jutikliai įvairiose pramonės srityse ir gali padidinti saugumą ir suteikti vietos taupymo pranašumų.

Table of Contents

List of Figures **8**
List of Tables **11**
List of Abbreviations **12**
Introduction **13**
1. Carbon fiber reinforced composite use as sensors in research **14**
1.1. Chapter summary 19
2. Testing methodology evaluation **26**
2.1. Chapter summary 34
3. Resistance measurement under dynamic and static loading **35**
3.1. Experiments 37
3.1.1. First test specimen 38
3.1.2. Second test specimen 40
3.1.3. Third test specimen 42
3.1.4. Fourth test specimen 44
3.2. Testing conclusions 48
3.3. Chapter summary 50
4. Economic evaluation of 3D printed CCFRP sensors **51**
4.1. Chapter summary 52
Conclusions **53**
List of References **54**
Appendices **57**
Appendix 1. Program code used to measure resistance periodically 57

List of Figures

Fig. 1. 3D printing technology classification [2] 14
Fig. 2. (a) The setup for the 3D printing of continuous fiber reinforced polymer composites. (b) Interface microstructures (c) Fracture pattern of fractured cross section of carbon fiber reinforced PLA composites [3] 15
Fig. 3. Axonometric projection of the airfoil (a) and the propeller (b) 3D models. UV-3D printed reproduction of the airfoil (c-f) and the propeller (g-j) 3D models based on the glass fiber (c, d, g, h) and carbon fiber (e, f, i, j) polymer composite formulations developed through research [3] 15
Fig. 4. (a, b) Photograph and (c) schematic of the strand retraction at the printing turn point [4] ... 16
Fig. 5. Sample: (a) scheme with FBG sensor locations, (b) surface photograph [5] 17
Fig. 6. Sample: (a) Photograph and scheme, (b) top view of the sample, and (c) cross-section of the sample; Sz—FBG sensor glued on the surface, Sw—FBG sensor embedded [6] 17
Fig. 7. Optimized fiber placement in CCFRP composite specimen [7] 18
Fig. 8. Schematic diagram showing the specimen dimensions and measurement method with electrical configuration. (a) Dog-bone shaped specimen, (b) rectangular specimen [9] 19
Fig. 9. Schematic showing the alignment of short fibers with the electric field in a UV photocurable resin system [10] 19
Fig. 10. Schematic showing the alignment of reinforcement along the applied magnetic field [10] 20
Fig. 11. MarkOne printer with separate nozzles for fiber filament and nylon filaments [10] 20
Fig. 12. Nano composite structure fabrication process. (a) – raw materials, (b) – micro compounder, (c) – screw extruder, (d) – extruded filament, (e) – 3D printer, (f) – printed specimens [11] 21
Fig. 13. SEM image of the 3D printed MWCNTs/ABS tensile test specimen fracture surface - 10% wt MWCNT loading showing MWCNT agglomeration [11] 21
Fig. 14. The experimental process of the integrated CFRP recycling technique via the additive manufacturing-based re-manufacturing method [12] 22
Fig. 15. Flexural test of the 3D printed rCFRP specimens: (a) dimensions, 3D print preview, and printout of the specimen; (b) flexural test setup; (c) representative stress-strain curve; (d) post-tested specimens showing failure modes [12] 22
Fig. 16. Applications of the 3D printed carbon fiber composite part from Stratasys: (a) car brake pedal; (b) gear in a transmission system [12] 23
Fig. 17. cheme of recycling and remanufacturing of 3D printed continuous carbon fiber reinforced thermoplastic parts (a). b) hot air gun, c) remolding nozzle, d) recycled impregnated filament, e) remanufacturing process [13] 23
Fig. 18. High tensile strength parts 3D printed using lose carbon fiber reinforced nylon filament [14] 24
Fig. 19. Flexible carbon fiber reinforced part with TPU matrix with electrostatic resistance [14] .. 24
Fig. 20. Nozzles used for 3D printing CFRP composite structures [15] 26
Fig. 21. Configuration of the test system for flexural test setup. [9] 26
Fig. 22. Variation of fractional change in resistance and stress with time during cyclic tensile loading for 100% fill density specimen [9] 27
Fig. 23. Complicated shape sensing element printing: (a) snake shape, (b) helix shape [9] 27
Fig. 24. Results of monitoring loads at different positions by electrical resistance measurement [16] 28
Fig. 25. Resistance and force versus time at the loading position of 80 mm for three loading cycles[16] 28

Fig. 26. Cyclic test held for 70 seconds without load [17] 29
Fig. 27. a) Graph of the electrical resistance (while the finger is bent); b) Graph of the electrical resistance (while the finger is straightened); c) Picture of 3D printed specimen; d) Resistance change curve of the wearable specimen (3%); e) Resistance change curve of the wearable specimen (9%) 29
Fig. 28. (a) the relationship between cyclic bending force and conductive resistivity of 3D printed CNTs-TPI (3%wt) and CNTs-TPI (9%wt) specimens; (b) Test process of cyclic bending parts [18] 30
Fig. 29. (a)Schematic of the set up used to determine the strain amplitudes of the cantilevers in the fatigue tests. (b)Schematic of the experimental setup of the dynamic bending fatigue test [19] 30
Fig. 30. (a) Tensile, (b) bending tests of CCFR-PLA [20] 31
Fig. 31. Schematic details of the multifunctional flexural-electrical characterization test [21] 31
Fig. 32. Failed test coupons after the multifunctional flexural-electrical characterization test [21]. 32
Fig. 33. Multifunctional flexural-electrical performance of test coupons at RTD: (a) 6207-00303; (b) 6207-00304; and (c) 6207-00305 [21] 32
Fig. 34. Schematic illustration of (a) carbon fiber bundle and (b) multiple CFRP strand specimens for the electromechanical test; (c) a home-made straining rig for piezo resistivity measurement [22] 33
Fig. 35. Scheme of designed jig and the constraint condition for the FEM analysis [23] 33
Fig. 36. Scheme for carbon fiber impregnation [24] 34
Fig. 37. Schematic of the 3D printer head used to print test specimens [25] 35
Fig. 38. Testing fixture: A – magnet, B – test specimen, C – fixture, D – electromagnet, E – measurement contact points 35
Fig. 39. Testing setup: 1 – testing fixture, 2 – Rigol DG1032Z arbitrary waveform generator, 3 – MMF LV 102 amplifier, 4 – Fluke 289 TRMS multimeter, 5 – Keithley 2614B source measure unit, 6 – computer 36
Fig. 40. Memmert UNB 400 universal oven 36
Fig. 41. Testing fixture placed inside the Memmert UNB 400 universal oven 37
Fig. 42. Rigol DG1032Z arbitrary waveform generator settings 37
Fig. 43. First test specimen 38
Fig. 44. Results of first test for the first specimen 38
Fig. 45. Short interval test results of the first test for the first specimen 39
Fig. 46. Results of the second test for the first specimen. 40
Fig. 47. Second test specimen 40
Fig. 48. Results of the first test for the second specimen 41
Fig. 49. Short interval test results of the first test for the second specimen 41
Fig. 50. Results of the second test for the second specimen 42
Fig. 51. Third test specimen 42
Fig. 52. Results of the first test for the third specimen 43
Fig. 53. Short interval test results of the first test for the third specimen 43
Fig. 54. Results of the second test for the third specimen 44
Fig. 55. Fourth test specimen 44
Fig. 56. Results of the first test for the fourth specimen 45
Fig. 57. Short interval test results of the first test for the fourth specimen 45
Fig. 58. Results of the second test for the fourth specimen 46
Fig. 59. Combined results of test No. 1 for all specimens 47

Fig. 60. Combined results of test No. 1 shorter time interval for all specimens 47
Fig. 61. Combined results of test No. 2 for all specimens 48
Fig. 62. Cost distribution of 3D printed CCFRP sensor development and manufacturing. 52

List of Tables

Table 1. Dynamic loading test results for all specimens 49

List of Abbreviations

Abbreviations:

ABS – Acrylonitrile Butadiene Styrene;
CCFRP – Continuous Carbon Fiber Reinforced Polymer;
CFRP – Carbon Fiber Reinforced Polymer;
CNT – Carbon Nano Tube;
FBG – Fibre Bragg Grating
FDM – Fuse Deposition Modelling;
MWCNT – Multi-Walled Carbon Nano Tube;
PLA – Polylactic Acid;
PEEK – Polyetheretherketone;
TPU – Thermoplastic Polyurethane.

Introduction

The use of 3D printing technology has revolutionized multiple manufacturing industries by allowing to manufacture new products rapidly, and incorporate new possibilities into the design. One of the most promising applications of 3D printing technology is continuous carbon fiber reinforced polymer (CCFRP) composites. CCFRP composites provide the required strength and stiffness with reduced weight of the parts. Especially for high performance applications in aerospace, automotive and biomedical industries.

However, CCFRP composites have numerous other benefits, such as excellent electrical and anti-corrosive properties, and reduced environmental impact during manufacturing of customized parts. One of the most promising electrical properties of CCFRP composites is piezo resistivity. It allows to incorporate them into sensing applications such as real-time monitoring of structural health, mechanical fatigue monitoring, and load sensing. The advancements in efficiency of 3D printing technology combined with piezo resistive properties of CCFRP composites create an opportunity to develop low-cost and high-performance sensors.

Previous research of 3D printed CCFRP composites has investigated numerous applications of the composite materials, however, application of piezo resistive properties in industry are still limited. This project aims to investigate the piezo resistive properties 3D printed CCFRP composites, including the fabrication of 0° and 0°-90° composite structures with various carbon fiber contents, testing their electrical resistance under static and dynamic loading, and evaluation of correlation between carbon fiber content and electrical resistance. Also, analysis of economic benefits when compared to traditional customized sensor development and manufacturing is performed.

The results of this project will show possible applications of 3D printed CCFRP composite structures, and cost-effectiveness of such sensors.

In conclusion, this project provides a comprehensive review of 3D printing technology impact on CCFRP composite manufacturing. The experiments show the piezoresistive properties of CCFRP composites when loaded cyclically and statically. The findings of this study will contribute to the growing interest of 3D printing technology use in CCFRP composite production and their application in various industries as load sensors.

Aim: To investigate the electrical resistance of 3D printed continuous carbons fiber reinforced composite structures.

Tasks:
1. to produce unidirectional 0° and 0°-90° composite structures with various carbon fiber content;
2. to test electrical resistance of composite structures under static loading;
3. to test electrical resistance of composite structures under dynamic loading;
4. to evaluate correlation between carbon fiber content and electrical resistance measured;
5. to evaluate economic benefits of 3D printed carbon fiber reinforced composite sensors

Hypothesis: Carbon fiber reinforced composite structures can be used as load sensors.

1. Carbon fiber reinforced composite use as sensors in research

3D printing technology has had a great impact on many industries in the past few years and its impact is increasing. One of the areas where the potential to use 3D printing is the highest is sensor production. 3D printing polymer matrices with fiber reinforcement greatly improves mechanical properties of the printed parts. Conductive reinforcement fibers, such as, carbon nanotubes are used to increase the strength of the parts, usually, without taking advantage of their electrical properties. Carbon fiber reinforced plastic composites are improved constantly. They are used in automotive, aviation, marine industries, and in various supporting parts. Main purpose of carbon fiber reinforcement is to increase mechanical strength of material. These composites are stronger and stiffer than metals, while their mass is around 60% of aluminium. These technical specifications make carbon fiber reinforced composites desirable in many applications. Main disadvantage of these fiber-polymer composites is increased unit price for manufacturing. Moreover, carbon fiber is conductive, that allows to use carbon fiber reinforced composite structures as shielding, electrical connections, or as electronic devices themselves.

Recent advancements in 3D printing technology have increased the interest in 3D printed composite development. In a recent overview study Yeong [1] analyzes the possible future applications and material development of 3D printed composites. The study highlights the mechanical properties of such materials, and their advantages when compared to metals, as well as, the cost-effectiveness of 3D printing technology for rapid prototyping. Continued development of 3D printing technologies is forecasted to gain interest and improve rapidly.

Also, numerous graphene-based composite materials are analyzed by Guo [2] in a study of recent advancements of 3D printing such materials. The study analyzes multiple 3D printing techniques, shown in Fig. 1. and their eligibility to manufacture 3D printed composites with graphene-based reinforcement. The study shows multiple recent 3D printing technology advancements being applied to create 3D printed graphene-based composites.

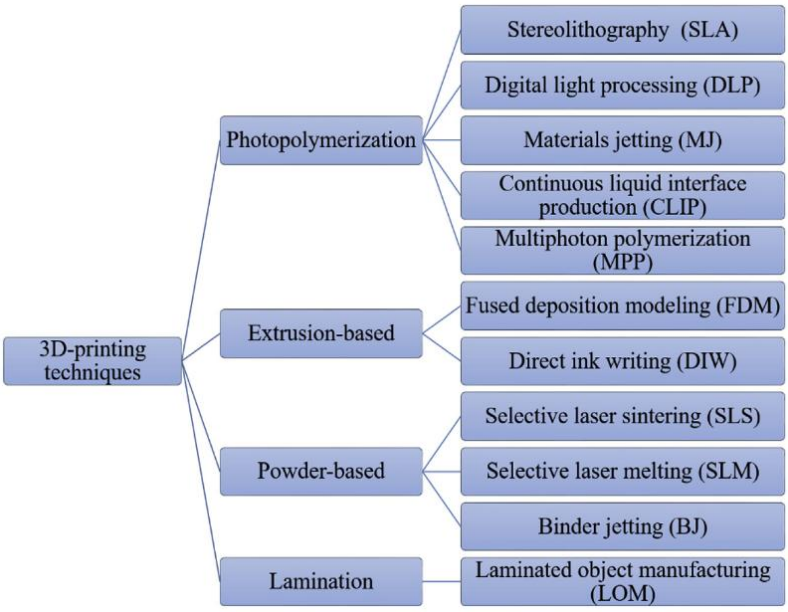

Fig. 1. 3D printing technology classification [2]

Carbon fiber reinforced polymer (CFRP) composites are widely used in various industries, including aerospace, automotive, biomedical and marine industries due to their high strength, low weight and exceptional corrosion resistance. CFRP are promising materials due to their high stiffness and strength-to-weight ratio. 3D printed CFRP production is a newly developed technology, that promises improved accuracy and precision when manufacturing complex shapes. Fig. 2. Shows schematic printing setup for CCFRP, interface microstructure and fracture pattern of CCFRP composites. Moreover, 3D printed CFRP has piezoresistive properties, meaning that they can be used as sensors at no additional cost. Wang's research [3] analyzes conductive materials, such as, carbon nanotubes inserted into a polymer matrix. Carbon nanotube reinforced polymer composite can detect mechanical strain applied to the part by changing its electrical resistance. This technology can potentially be used in biomedical industry as integrated sensors for prosthetics, implants and personalized medical devices. Also, it has potential applications in aerospace industry to monitor the integrity of the spacecraft or aircraft. Fig. 3. shows glass and carbon fiber reinforced 3D printed polymer parts using the polymer formulation developed during research by the authors. The structures are printed using a UV reactive resin

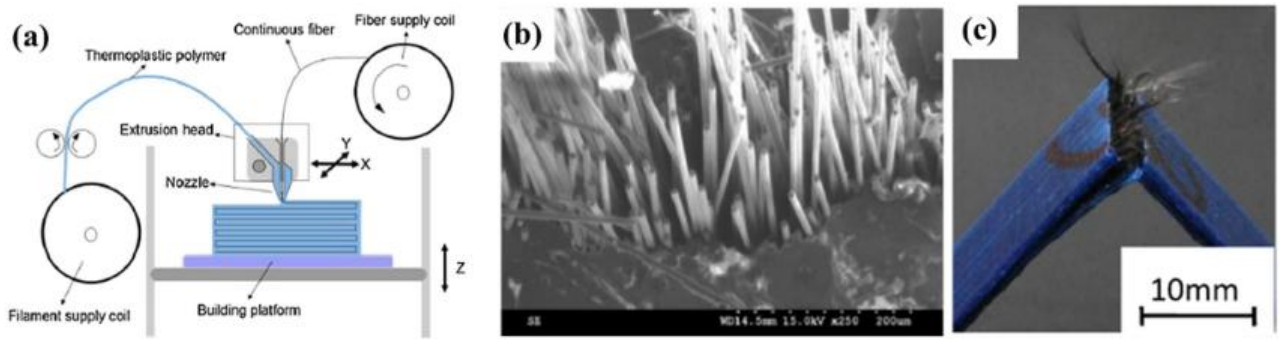

Fig. 2. (a) The setup for the 3D printing of continuous fiber reinforced polymer composites. (b) Interface microstructures (c) Fracture pattern of fractured cross section of carbon fiber reinforced PLA composites [3]

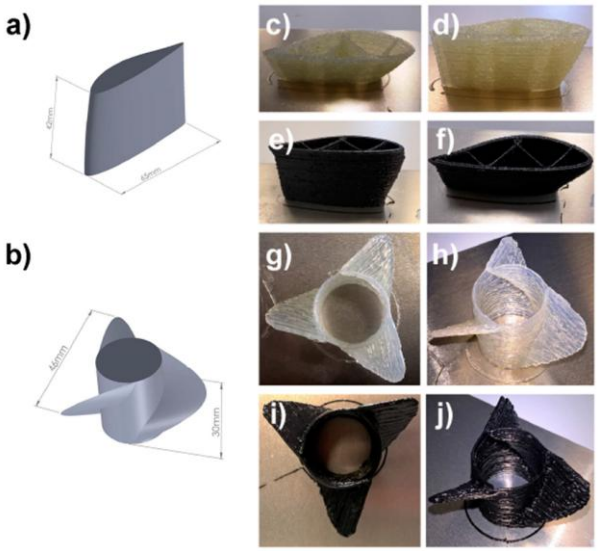

Fig. 3. Axonometric projection of the airfoil (a) and the propeller (b) 3D models. UV-3D printed reproduction of the airfoil (c-f) and the propeller (g-j) 3D models based on the glass fiber (c, d, g, h) and carbon fiber (e, f, i, j) polymer composite formulations developed through research [3]

The development of continuous carbon fiber reinforces polymer (CCFRP) materials has been gaining attention in recent years. According to Zhang's research [4], CCFRP sensors have multiple advantages compared to traditional sensors, including improved sensitivity, durability and flexibility. The article explains how 3D printing technology enables the production of complex shapes and geometries, thus increasing the sensitivity of the sensors. Fig. 4. Shows the test of retraction of the fibers for a complex shape after printing. Moreover, CCFRP material has high strength-to-weight ratio, which improves the durability of the sensors. Furthermore, the flexibility of CCFRP composites allow the sensors to conform to irregular surfaces, increasing the range of sensor motion without requiring more space, and expanding the range of possible applications. The research also suggests that 3D printing technology allows for creation of custom sensors tailored to the required properties of the application. The ability to customize properties of the sensors increases the number of its potential use cases in different environments with improved accuracy and precision. The article concludes that 3D printed CCFRP technology has promising potential for the advancement of sensing technology.

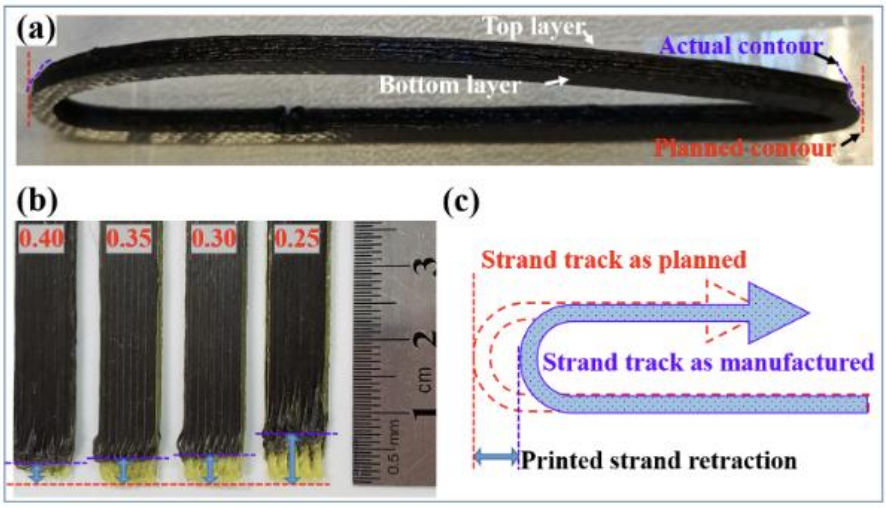

Fig. 4. (a, b) Photograph and (c) schematic of the strand retraction at the printing turn point [4]

Moreover, sensor development is a crucial aspect in various scientific and engineering fields. In a recent study by Shafighfard and Mieloszyk [5] the authors conduct an experiment with CCFRP composite part with integrated fiber Bragg grating sensors, the placement of the sensors inside the part is shown in Fig. 5. Continuous carbon fiber reinforced polymer sensors show numerous advantages such as high stiffness, low weight, and corrosion resistance, making them desirable in automotive and aerospace industry applications. 3D printing technology allows to create required shapes with lower production costs and lower production time, when compared to regular sensors with custom properties. CCFRP sensor application has been tested in various scenarios, including structural health monitoring and vibration detection, showing high sensitivity and accuracy when detecting changes and vibrations. The study concludes, that the combination of 3D printing technology and CCFRP composite material has great potential for future sensor development.

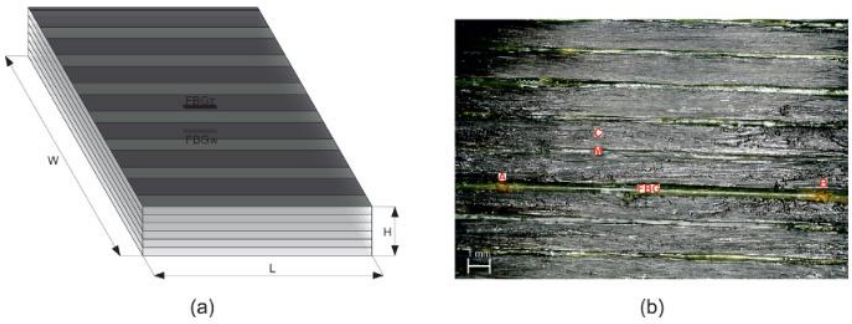

Fig. 5. Sample: (a) scheme with FBG sensor locations, (b) surface photograph [5]

Also, recent advancements in 3D printing technology have enabled the creation of CCFRP structures with unique mechanical and electrical properties. Shafighfard and Mieloszyk's research [6] analyzes the influence of temperature change in CCFRP samples. The authors found that CCFRP samples have a linear response to loading when measuring electrical resistance change, which is critical for sensor accuracy. The samples showed great sensitivity to strain, proving that the material is suitable for sensor production. The research analyzes CCFRP composite 3D printed specimens with glued surface sensors, as well as, embedded sensors inside the specimen. Fig. 6. shows sensor placement in the specimens. The authors investigate the mechanical strain resistance of CCFRP composite parts in different temperatures. Also, researchers found that CCFRP sensors have numerous advantages, including low manufacturing cost, ease of fabrication, and shape and geometry advantages caused by 3D printing technology. 3D printing technology improves sustainability and lowers environmental impact because the material waste is minimized, and usage of thermoplastics improves recyclability of the parts. Overall, 3D printed CCFRP composites have a wide range of application as a promising sensing material.

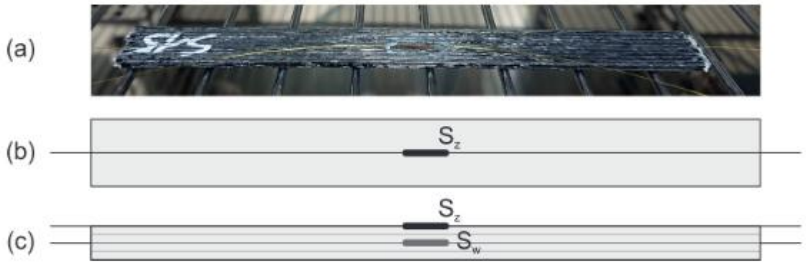

Fig. 6. Sample: (a) Photograph and scheme, (b) top view of the sample, and (c) cross-section of the sample; Sz—FBG sensor glued on the surface, Sw—FBG sensor embedded [6]

Furthermore, various applications of CCFRP including sensors have been in development. Liu [7] investigates the potential of 3D printed CCFRP as a sensor material. The article investigates several 3D printing techniques to achieve specific geometries of self-sensing specimens, as well as different fiber placement to incorporate sensing properties into required areas, while leaving unnecessary parts free of fiber content. Fig. 7. shows fiber trajectory optimized sensor printing path. The research shows that CCFRP material exhibited excellent mechanical and electrical properties, making it suitable for sensing applications. The researchers also found that, changing 3D printing properties, such as, printing temperature and speed greatly influenced the mechanical and electrical properties of the final material. Also, the experiments conducted it the article shows that the material can detect changes in temperature and strain with high sensitivity and accuracy. The study concludes that 3D printed CCFRP is a suitable material for sensor production.

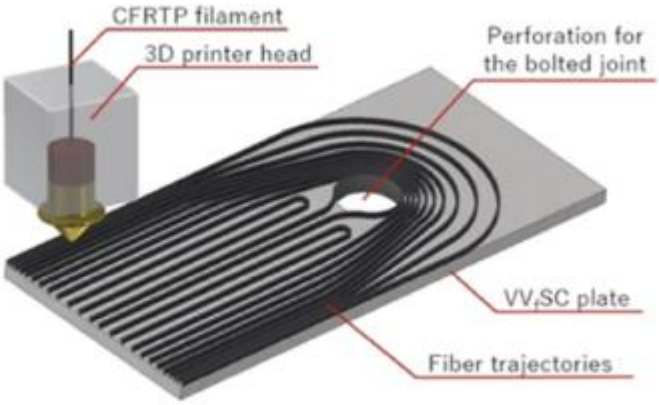

Fig. 7. Optimized fiber placement in CCFRP composite specimen [7]

An article by Biswas [8] in Fiber-Reinforced Polymers Processes and Applications by Raja shows that CCFRP can act as a sensor due to its piezoresistive properties. Piezoresistive materials react to applied strain by changing their electrical resistance, making them ideal to use as sensors. The chapter in the book analyzes applications of nano-engineered fiber-based polymer composites, it describes their application as sensors due to their piezoresistive properties. By 3D printing CCFRP structures it is possible to produce highly accurate sensors that have an optimized shape, and mechanical and electrical properties for each unique application with high production rate, as well as, low material waste and minimal costs for tooling. Advancements in 3D printing technology are revolutionizing the structural health monitoring field, as the sensors are integrated directly into the structures, providing real-time feedback on their performance. Also, the cost-effectiveness of 3D printing allows these sensors to be produced at a lower cost than traditional sensors making them a suitable option for widespread applications.

Recently researchers started exploring 3D printing technology to fabricate CFRP-based sensors. These sensors have shown great potential in strain, deformation sensing, and self-health monitoring applications. Such sensors are studied by Luan [9], the researchers developed a fabrication technique to 3D print CCFRP sensors, and analyzed their performance in measuring strain and deformation. 3D printed CCFRP sensors showed great stability, durability, as well as, accuracy and precision while cyclically loaded. Fig. 8. shows specimen dimensions and continuous carbon fiber strand placement in the specimens. The development of 3D printed CCFRP sensors has the potential to provide cost-effective and efficient method of monitoring health of CFRP structures and measuring the materials performance. It shows a potential to improve safety and reliability in multiple industries, such as, aerospace, automotive, and sports.

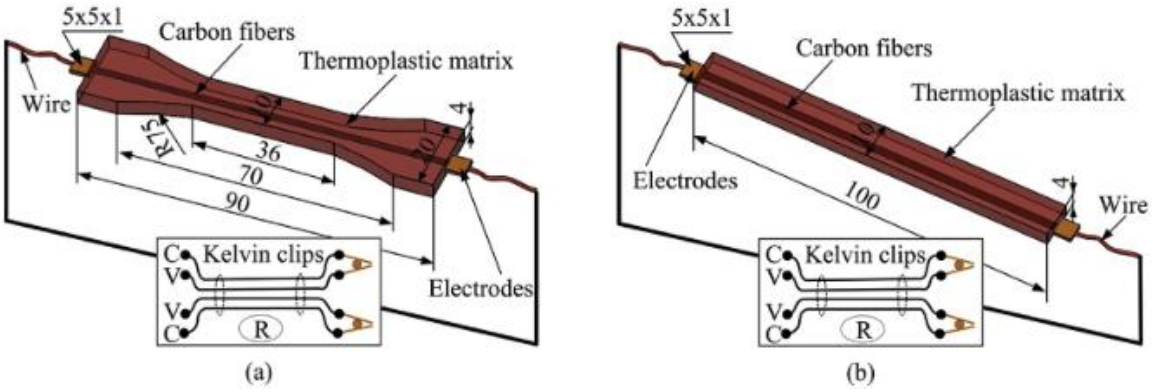

Fig. 8. Schematic diagram showing the specimen dimensions and measurement method with electrical configuration. (a) Dog-bone shaped specimen, (b) rectangular specimen [9]

Moreover, a review of carbon fiber reinforced composite printing techniques and material properties was done by Adil [10]. The article shows 3D printing technologies that can be used in CFRP composite production, including fuse deposition modeling, selective layer sintering and stereolithography. Also, the authors analyze field assistance techniques for loose fiber reinforced composites. These techniques align the fibers in the printed parts during the printing process, for instance, using an electric field to align the fibers in photocurable resin as shown in Fig. 9, as well as, applying a magnetic field to the print plate of fuse deposition modeling printer to align the fibers in the last layer that was printed as shown in Fig. 10. Furthermore, the article analyzes continuous carbon fiber reinforced composite printing techniques, one of which is shown in Fig. 11. The shown method uses two nozzles, the first for the continuous carbon fiber strand, the second for nylon filament. The authors state some possible applications for 3D printed CFRP composites, mainly focusing on improved mechanical properties for aerospace industry. Also, there are some disadvantages presented in the article, for instance, voids in the printed parts, increase cracking potential due to the boundary between the fibers and the matrix material.

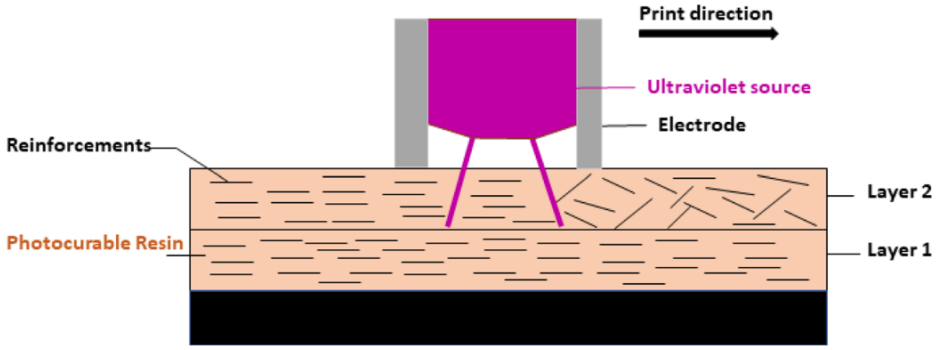

Fig. 9. Schematic showing the alignment of short fibers with the electric field in a UV photocurable resin system [10]

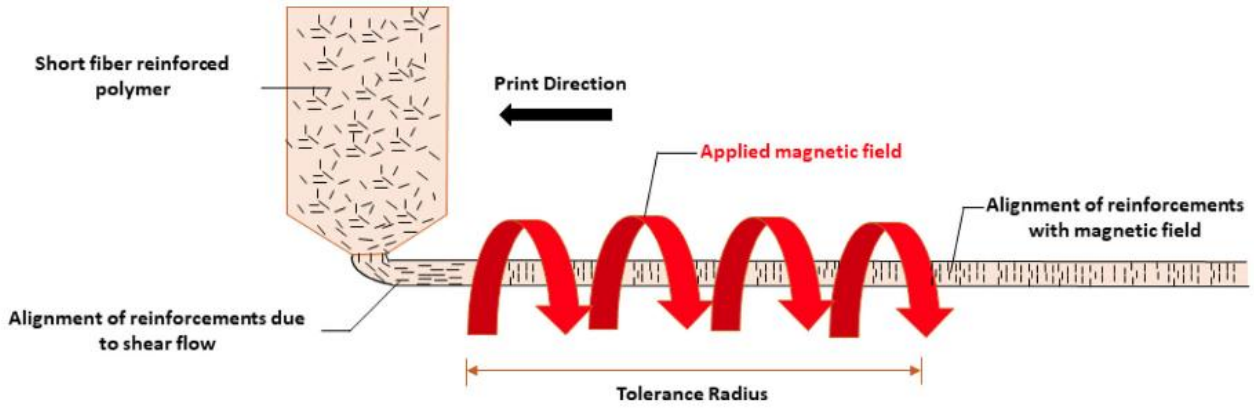

Fig. 10. Schematic showing the alignment of reinforcement along the applied magnetic field [10]

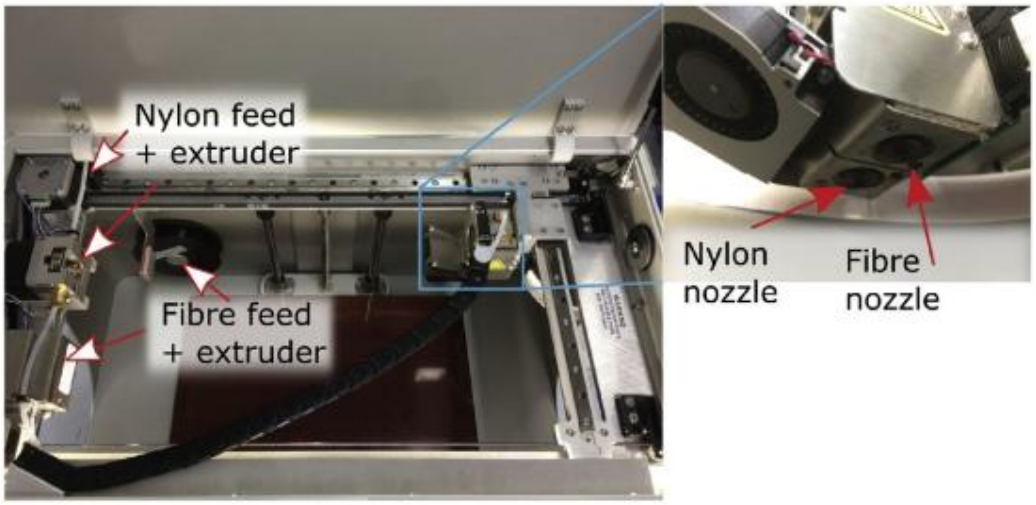

Fig. 11. MarkOne printer with separate nozzles for fiber filament and nylon filaments [10]

Furthermore, an article by Sezer [11] analyzes the improved mechanical and electrical properties of carbon nanotube reinforced composite in ABS matrix. The research shows the process of manufacturing ABS filament with carbon nanotube particles. The screw extruder is used to mix ABS pellets with carbon nanotube powder, the process is shown in Fig. 12. The research analyzes the breakage of the specimens after destructive mechanical testing, showing the imperfections of the specimens due to the 3D printing process and the inconsistencies of the extruded filament. The tested specimens were photographed using a scanning electron microscope to see the structure of the laid filament and the distribution of carbon nanotubes inside the printed specimens. Fig. 13. shows a scanning electron microscope image of a carbon nanotube agglomeration inside the printed part, showing the inconsistency of the mixing and extruding process during the filament fabrication.

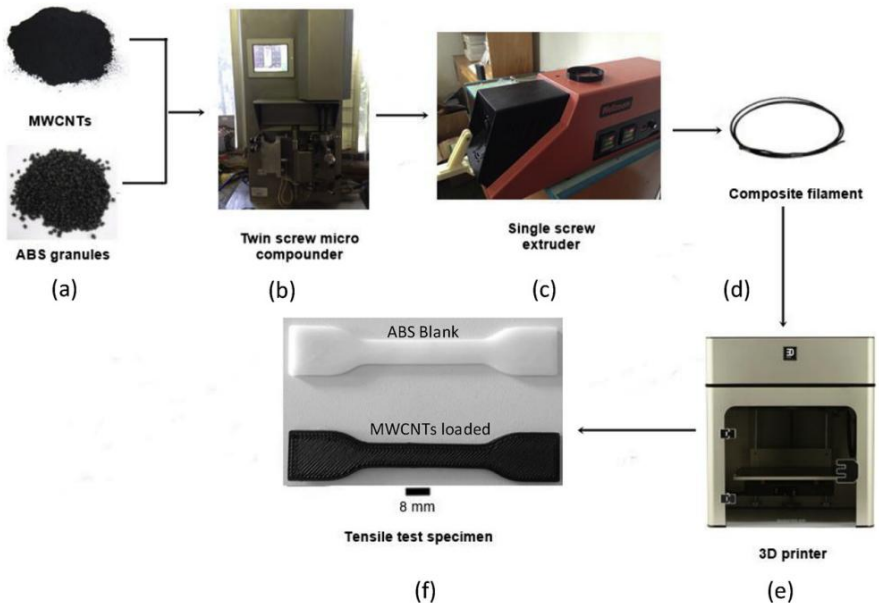

Fig. 12. Nano composite structure fabrication process. (a) – raw materials, (b) – micro compounder, (c) – screw extruder, (d) – extruded filament, (e) – 3D printer, (f) – printed specimens [11]

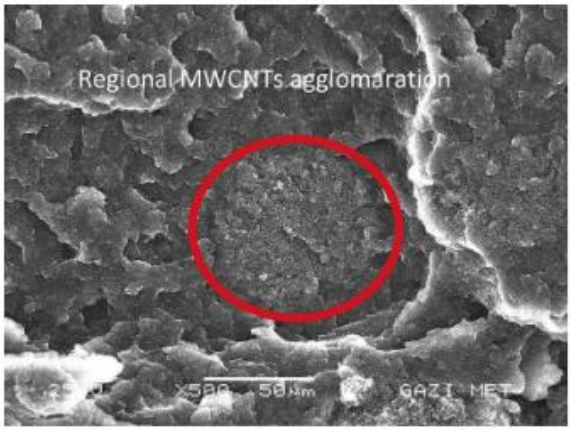

Fig. 13. SEM image of the 3D printed MWCNTs/ABS tensile test specimen fracture surface - 10% wt MWCNT loading showing MWCNT agglomeration [11]

An environmentally friendly solution is suggested by Liu [12] in his research on carbon fiber reinforced 3D printed composite parts by using reclaimed carbon fibers from traditional carbon fiber composite manufacturing waste. The research describes the methodology for manufacturing the filament from waste carbon fibers and printing the test specimens for strength testing. Fig 14. shows the process of manufacturing the filament and printing the specimens. The tests on the specimens showed a minor degradation of mechanical properties of reclaimed carbon fiber reinforced filament specimens when compared to virgin carbon fiber reinforced filaments. Fig. 15. shows the testing procedure and results for bending test of virgin and reclaimed carbon fiber reinforced composite filament and pure PEEK test specimen. The results show that reclaimed carbon fiber reinforced filament has improved mechanical properties when compared to pure PEEK filament specimens, but does not reach the performance of virgin carbon fiber reinforced PEEK filament specimens. Using this king of process in 3D printed carbon fiber reinforced composite sensor production would reduce the impact on the environment, while reducing the cost of carbon fiber required for filament production. The electrical properties of these specimens were not evaluated in this research; however,

similar tests can be performed while measuring the resistance of the specimens to evaluate their performance. Fig. 14. shows some applications for 3D printed carbon fiber reinforced composites.

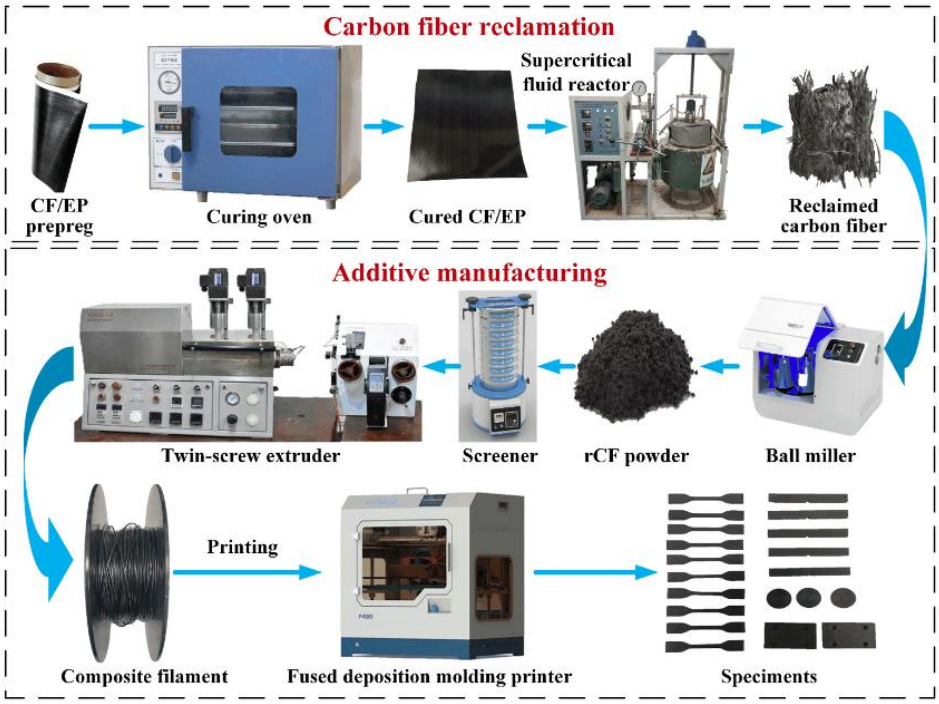

Fig. 14. The experimental process of the integrated CFRP recycling technique via the additive manufacturing-based re-manufacturing method [12]

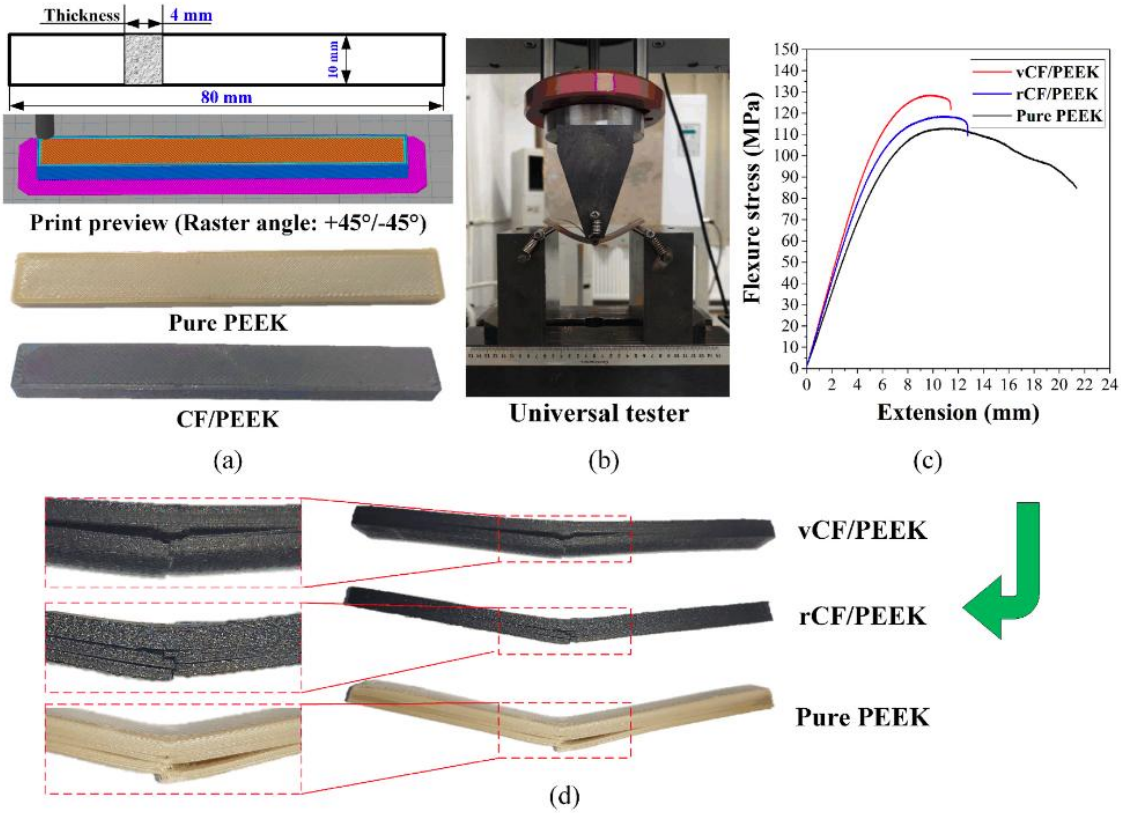

Fig. 15. Flexural test of the 3D printed rCFRP specimens: (a) dimensions, 3D print preview, and printout of the specimen; (b) flexural test setup; (c) representative stress-strain curve; (d) post-tested specimens showing failure modes [12]

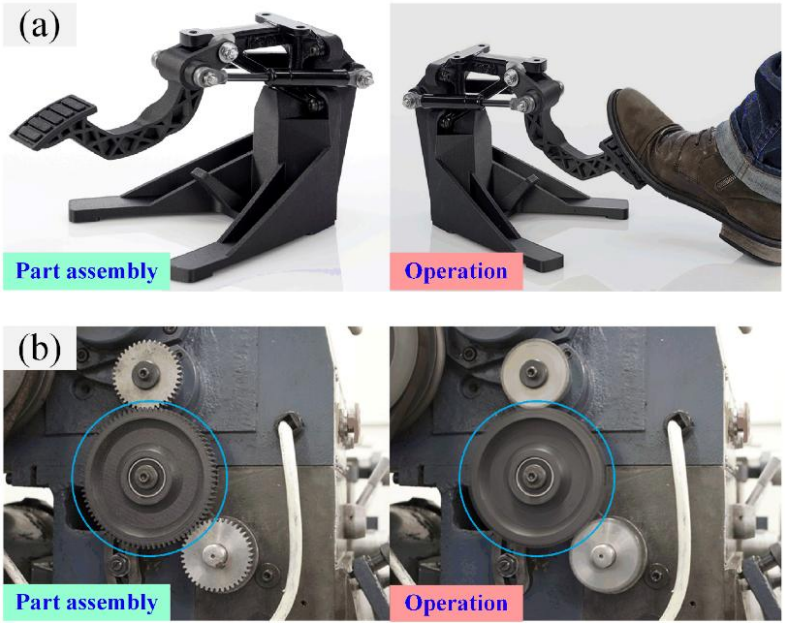

Fig. 16. Applications of the 3D printed carbon fiber composite part from Stratasys: (a) car brake pedal; (b) gear in a transmission system [12]

Another article, suggesting a recycling process for already printed continuous carbon fiber parts was done by Tian [13]. The article shows a process to remelt the printed parts and extract the continuous carbon fiber to be re-extruded through a nozzle and spooled onto a bobbin. The remelted filament can be used again, however a reduction in mechanical and electrical properties may occur, due to the shape of the part and damage to the fiber strand during the original printing process. The recycling process is shown in Fig. 17.

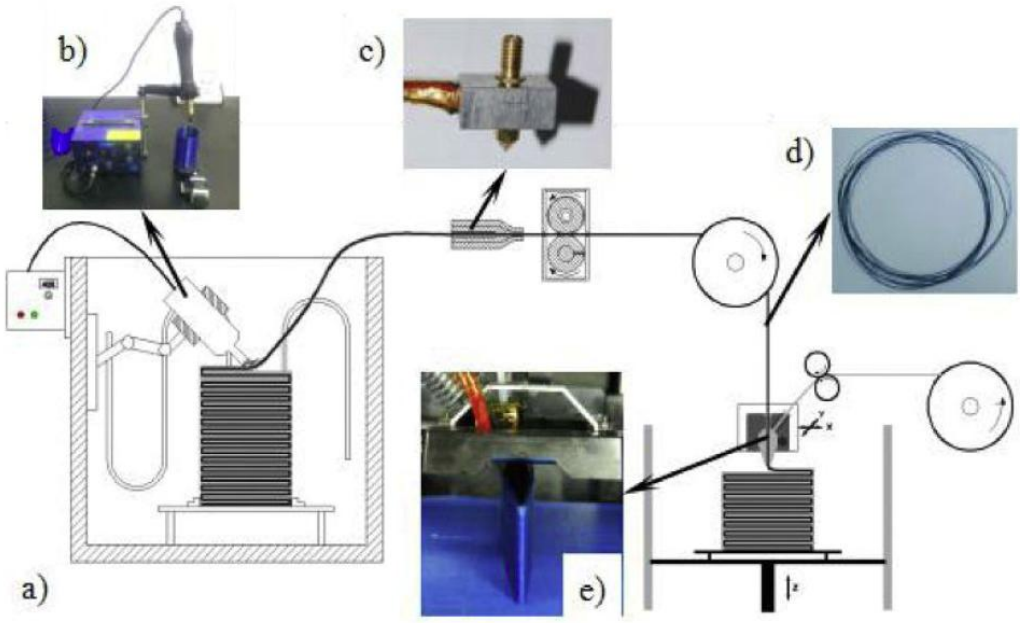

Fig. 17. cheme of recycling and remanufacturing of 3D printed continuous carbon fiber reinforced thermoplastic parts (a). b) hot air gun, c) remolding nozzle, d) recycled impregnated filament, e) remanufacturing process [13]

1.1. Commercially available carbon fiber reinforced filaments

There are multiple commercially available filament and resin options with carbon particle or continuous carbon fiber reinforcement. An overview of 3D printing filaments with carbon fiber reinforcement in FDM printing is done by Carolo [14]. The article compares multiple commercially available filaments, highlighting their mechanical properties, printer requirements and other benefits. The main focus of the article is on carbon fiber reinforced nylon filament from multiple manufacturers, the nylon-based filament improves mechanical properties of 3D printed parts while maintaining excellent dimensional accuracy of ± 0.02 mm. Fig. 18. shows parts printed in lose carbon fiber reinforced nylon filament, the material is chosen for its improved mechanical properties, mainly tensile strength. Also, other materials are compared in the article, such as, PLA, ABS and TPU reinforced with carbon fibers. Different matrix materials for carbon fiber reinforced composites allow them to be applied in different scenarios, for instance a flexible TPU-based filament is produced by Smart Materials that improves the electrical properties of flexible parts. The application described in the article is printing flexible parts that are resistant to electrostatic discharge, making them ideal for flexible shielding. Fig. 19. shows a flexible TPU part with carbon fiber reinforcement.

Fig. 18. High tensile strength parts 3D printed using lose carbon fiber reinforced nylon filament [14]

Fig. 19. Flexible carbon fiber reinforced part with TPU matrix with electrostatic resistance [14]

1.2. Chapter summary

Overall, continuous carbon fiber reinforced polymers are proven to be suitable for sensing applications in numerous industries, such as aerospace, automotive, biomedical, and medical devices.

The linear relation of strain applied to the material and change in electrical resistance allows for production of sensors using these materials. The 3D printing technology allows for complex shapes and geometries of sensors to be manufactured with low costs and environmental impact. The conducted experiments in multiple studies show high accuracy and precision. Recent advancements in 3D printing technology and composite material science show great potential for customized sensor production.

2. Testing methodology evaluation

Continuous carbon fiber reinforce composites are researched extensively in recent years due to their mechanical and electrical properties. One such research was done by Todoroki [15] investigating the tensile properties of CCFRP composites. The article shows the printing methodology for CCFRP composite test specimens using two separate printing nozzles in FDM 3D printer (shown in Fig. 20.). The authors evaluate the tensile performance of multiple printing lay-up directions

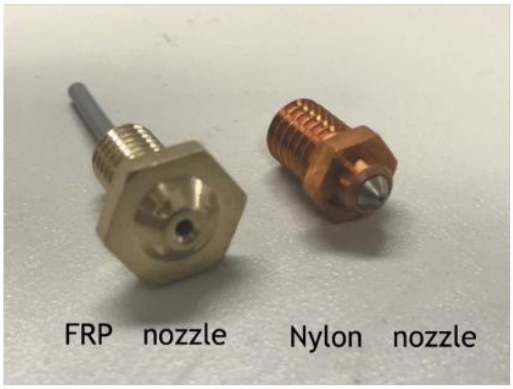

Fig. 20. Nozzles used for 3D printing CFRP composite structures [15]

Furthermore, carbon fiber reinforced composites are studied extensively, trying to find new ways they can be used in different fields. One of the fields of research is creating 3D printed parts with carbon fiber reinforcement, and analyzing their properties. One example of such printed parts is shown in Luan's research [9] of continuous carbon fiber reinforced thermoplastic based on dual-material 3D printing integration process. The research analyses the change in mechanical and electrical properties of the composite material when compared to thermoplastic. The article shows the equipment used to print the test specimens, testing methodology used, and the result analysis. The focus of the study is to analyze the relation between mechanical loading and electrical resistance of the carbon fiber strands inside the specimen. The testing setup used in the study is shown in Fig. 21., the tests were conducted using three-point bending testing methodology, while using a cyclical load. Results show that the change in electrical resistance is directly related to the mechanical stress inside the specimen. Fig. 22. Shows the fractional change in resistance and stress with the time during cyclic loading.

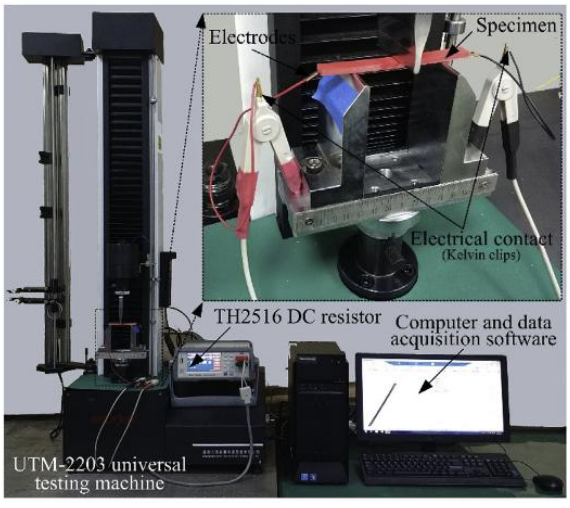

Fig. 21. Configuration of the test system for flexural test setup. [9]

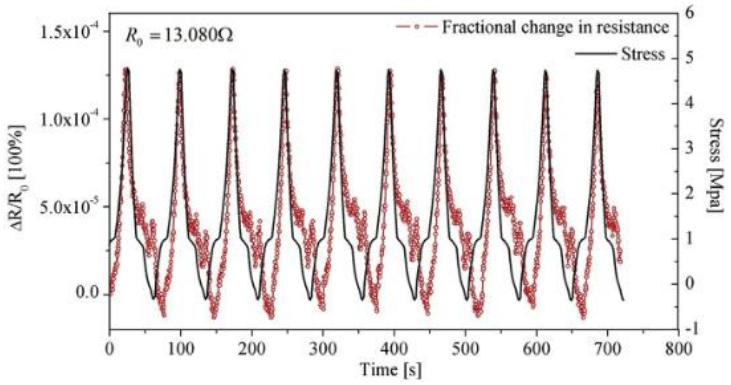

Fig. 22. Variation of fractional change in resistance and stress with time during cyclic tensile loading for 100% fill density specimen [9]

Moreover, using the method described in Luan's research it is possible to create intricate shapes of sensing elements shown in Fig. 23. These sensing elements can be used inside other parts, where conventional sensors are not viable due to space, structural, or appearance concerns. The sensing elements can be completely hidden inside the printed parts, only having the measurement contact points on the outside.

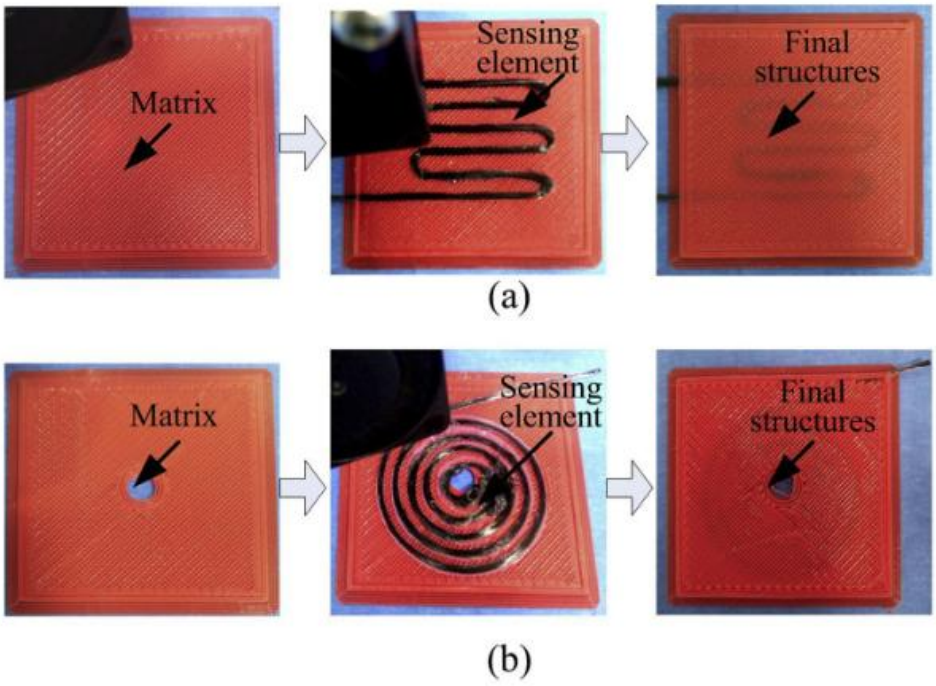

Fig. 23. Complicated shape sensing element printing: (a) snake shape, (b) helix shape [9]

In addition, Luan's research of self-sensing of loads in continuous carbon fibers-embedded 3D-printed polymer structures using electrical resistance measurement [16] details formulae to calculate the electrical resistance in relation to the load applied to the specimen with minimal error of less than 1.3 % (shown in Fig. 24). The formulae provide with accurate results when compared to the testing specimens. This study analyses positional loads and shows that real-time data can be observed during loading. Fig. 25. shows the relation between the force applied and electrical resistance inside the carbon fiber strand during cyclical loading of the specimen. Although, the

calculation cannot be performed for all CCFRP applications due to the differences in 3D printing lay-up, the proof of the results shows, that such formulae can be developed.

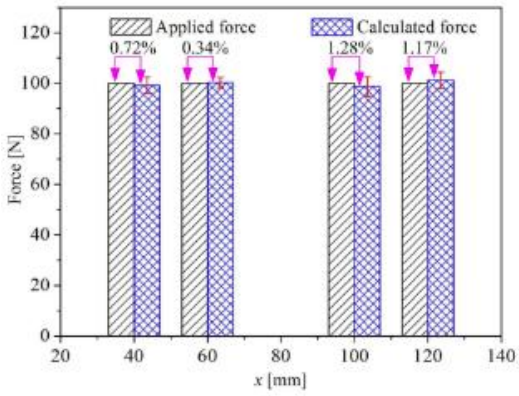

Fig. 24. Results of monitoring loads at different positions by electrical resistance measurement [16]

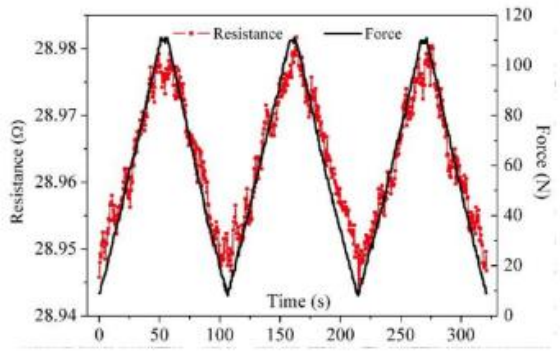

Fig. 25. Resistance and force versus time at the loading position of 80 mm for three loading cycles[16]

However, Iizuka's research describes the non-linear behavior mechanism of change in electrical resistance on 3D printed carbon fiber / PA6 composites during cyclic testing [17]. The research results show that loading and unloading gauge factors are different from each other, the unloading gauge factor does not reach the value of loading gauge factor, thus reducing the resulting electrical resistance with each loading cycle. Fig. 26. shows the reduction of electrical resistance in relation with the number of cycles. The research concluded that the viscoelasticity of the polymer causes the reduction of electrical resistance between loading cycles. The reduction of electrical resistance depends on the speed of testing, the higher the loading frequency, the greater the reduction of resistance in the specimen.

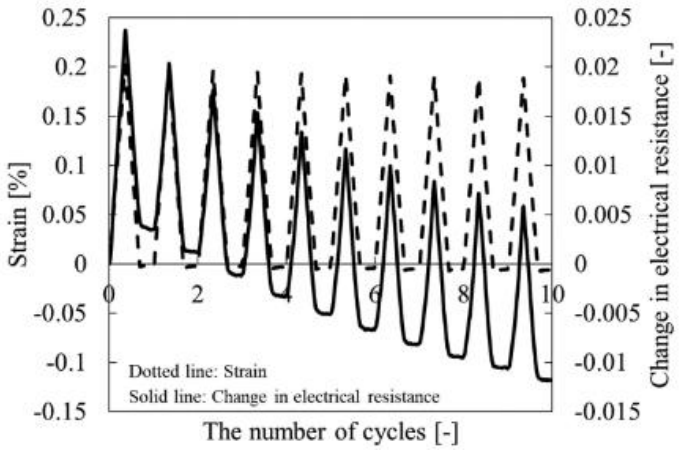

Fig. 26. Cyclic test held for 70 seconds without load [17]

Furthermore, Ye's research [18] of carbon nanotubes reinforced thermoplastic polyimide composites with controllable mechanical and electrical properties analyses the effect of different ratios of carbon nanotube content in 3D printed specimens. This study shows the methodology developed to produce the filament used for specimen printing, the testing methodology, and microscopic structure of the printed parts with different ratios of carbon nanotube content. Fig. 27. shows the relation of cyclic loading force and electrical resistance, and testing apparatus used to perform the tests. Also, the researchers have tested a coiled spiral part with different carbon fiber content worn on the finger (Fig. 28.), that showed a change in resistance when the finger was bent, showing another possible application of such sensors.

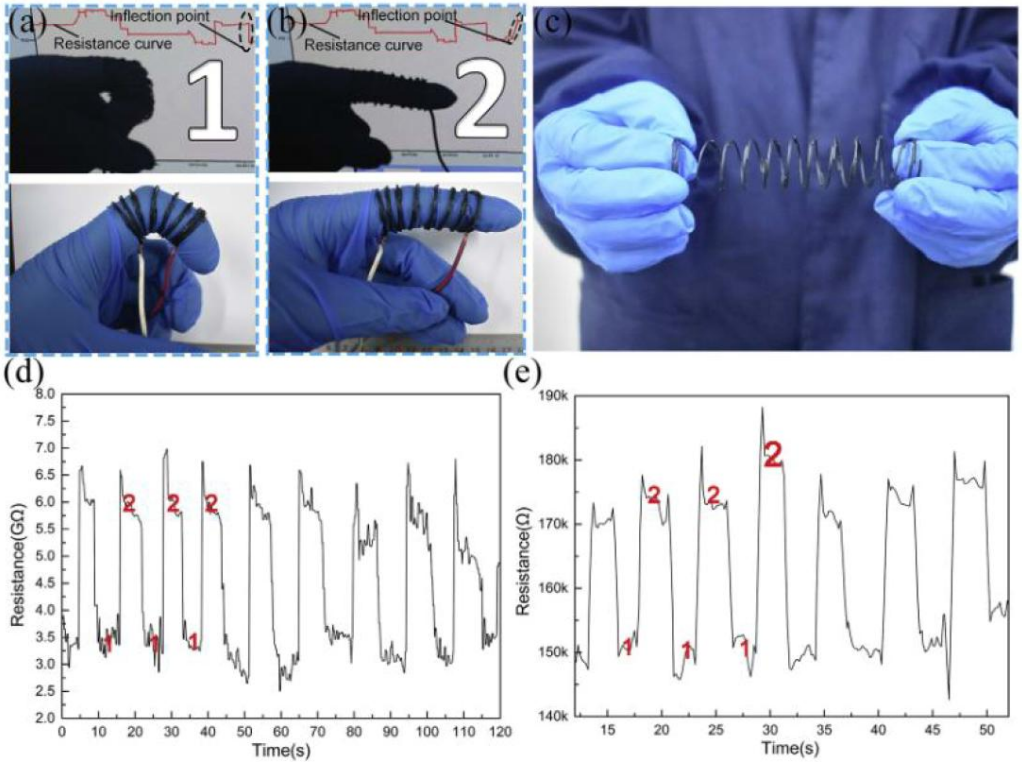

Fig. 27. a) Graph of the electrical resistance (while the finger is bent); b) Graph of the electrical resistance (while the finger is straightened); c) Picture of 3D printed specimen; d) Resistance change curve of the wearable specimen (3%); e) Resistance change curve of the wearable specimen (9%)

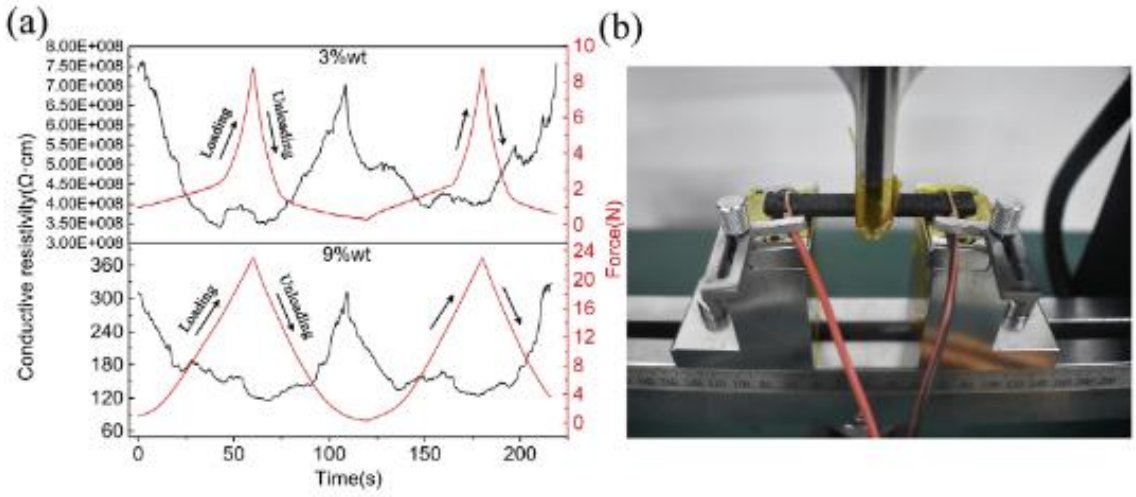

Fig. 28. (a) the relationship between cyclic bending force and conductive resistivity of 3D printed CNTs-TPI (3%wt) and CNTs-TPI (9%wt) specimens; (b) Test process of cyclic bending parts [18]

Moreover, a cantilever beam bending test was performed in Zheng's research [19] evaluating fatigue reliability of flexible nanoscale films. The research uses a waveform function generator and power amplifier to power an electromagnet which affects the sample. The test was conducted to evaluate mechanical properties of the samples; however, the testing setup can be adapted to measure electrical resistance change during cyclical loading of the specimens. Schematic view of strain amplitude determination setup and experimental setup is shown in Fig. 29.

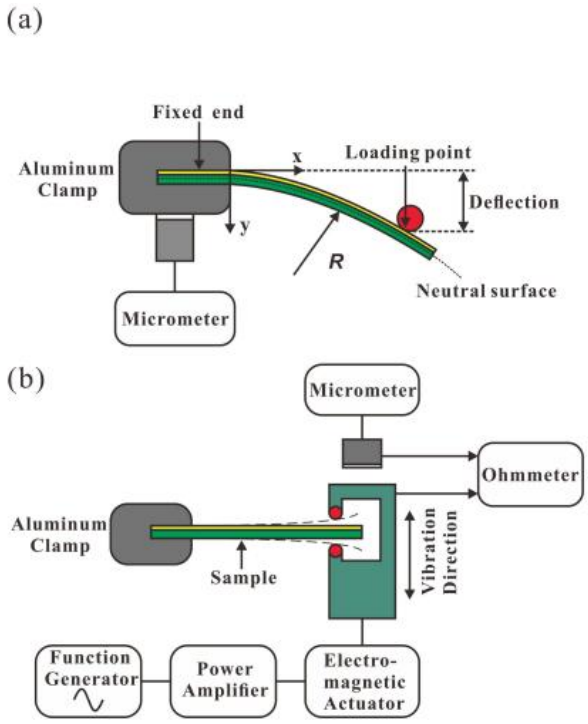

Fig. 29. (a)Schematic of the set up used to determine the strain amplitudes of the cantilevers in the fatigue tests. (b)Schematic of the experimental setup of the dynamic bending fatigue test [19]

Another example of three-point bending and tensile tests is shown in Heidari-Rarani's research on continuous carbon fiber reinforced 3D printed composite mechanical properties. The researchers analyze the mechanical stress and strain resistance of continuous carbon fiber reinforced composites.

The testing methodology can be adapted to measure electrical resistance during the tests. The testing setups for tensile and three-point bending tests are shown in Fig. 30.

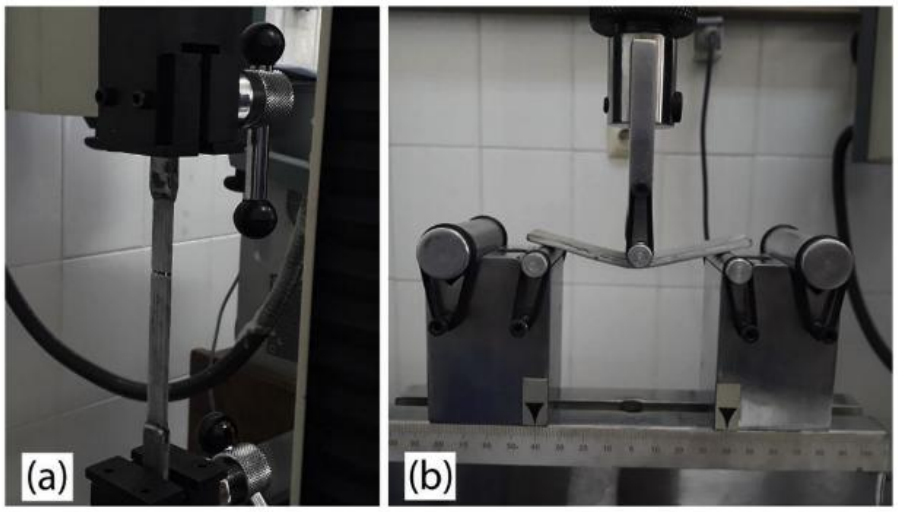

Fig. 30. (a) Tensile, (b) bending tests of CCFR-PLA [20]

Additionally, a study of coupled flexural-electrical evaluation of additively manufactured multifunctional composites was conducted by Ghimire [21]. The article explains the process of 3D printing CCFRP test specimens using a Markforged FDM printer with two nozzles. The electrical properties testing was conducted using three-point bending test as shown in Fig. 31. The tests were conducted until the test specimens failed as shown in Fig. 32, the results of the tests are shown in Fig. 33. The test results concluded that the change in resistance varies between each layer of the test coupon, similar to traditional carbon fiber composites, however, it also showed a reduces delamination effect due to 3D printing process.

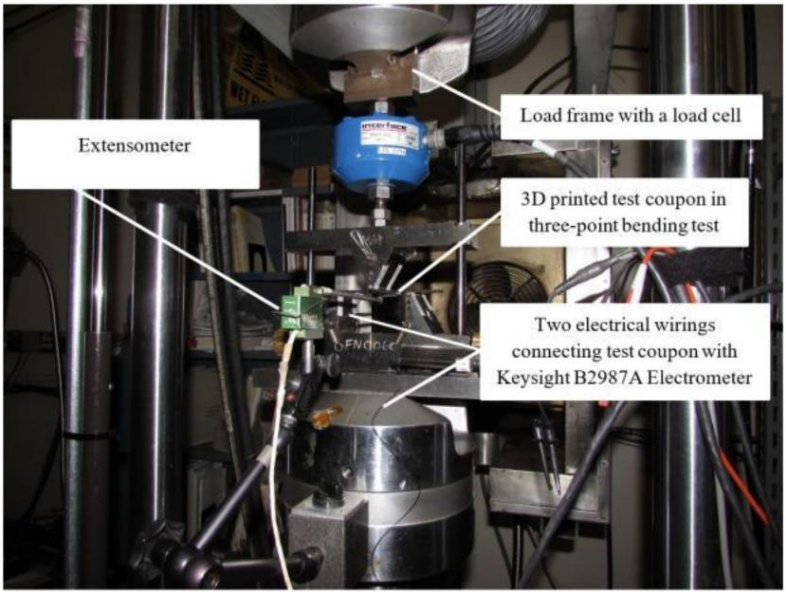

Fig. 31. Schematic details of the multifunctional flexural-electrical characterization test [21]

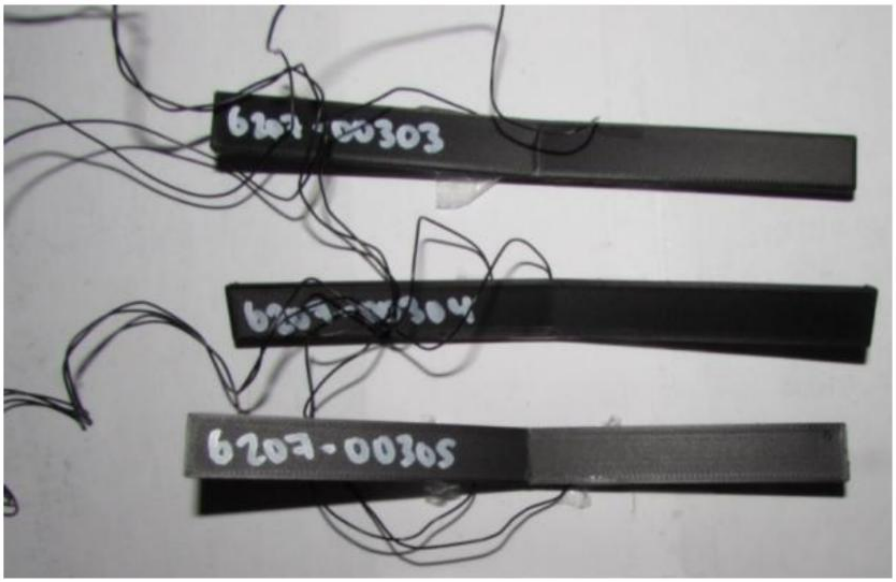

Fig. 32. Failed test coupons after the multifunctional flexural-electrical characterization test [21]

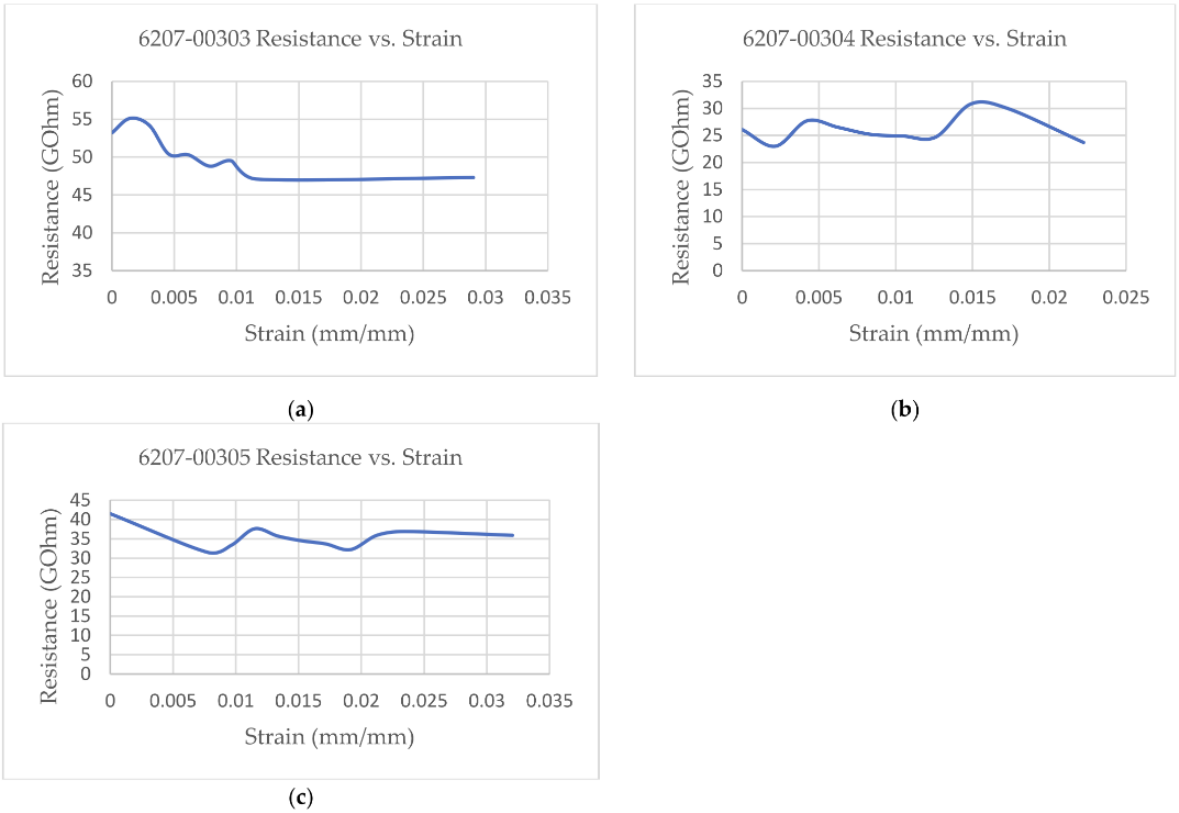

Fig. 33. Multifunctional flexural-electrical performance of test coupons at RTD: (a) 6207-00303; (b) 6207-00304; and (c) 6207-00305 [21]

Continuing, a different experimental study was conducted by Kalashnyk [22] where the tensile test was conducted while monitoring the electrical resistance of the 3D printed specimen. The study showed that while the specimens are under tensile stress, the internal fibers breaking are increasing the electrical resistance of the specimens. The self-monitoring characteristic of CCFRP material is investigated. The testing apparatus is shown in Fig. 34. The tests conducted during the experiment show that CCFRP composites can be used to monitor their own health by measuring the electrical resistance before the application and after.

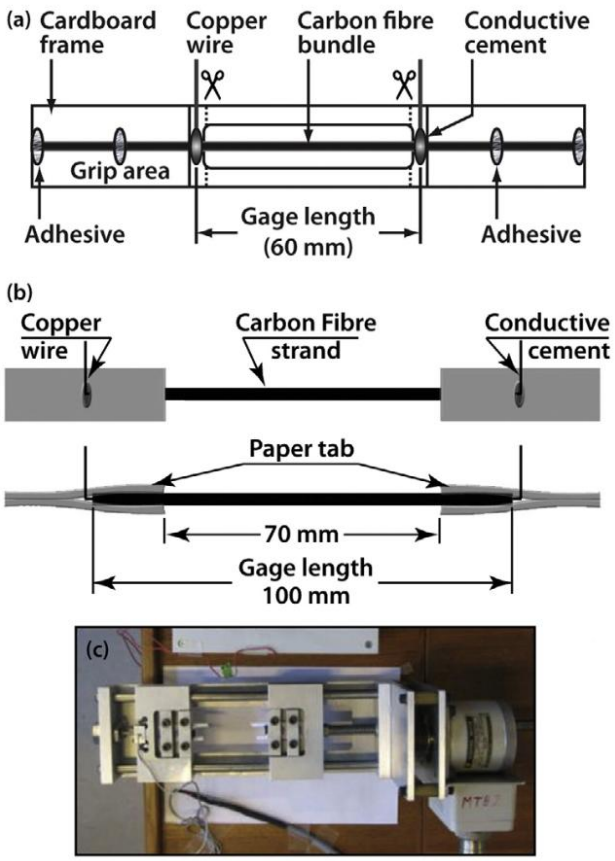

Fig. 34. Schematic illustration of (a) carbon fiber bundle and (b) multiple CFRP strand specimens for the electromechanical test; (c) a home-made straining rig for piezo resistivity measurement [22]

Furthermore, a comprehensive study of mechanical strength degradation of the curved sections of 3D printed CCFRP specimens was conducted by Shiratori [23]. The testing methodology includes curved section loading to observe the fatigue of CCFRP specimens. The testing methodology scheme is shown in Fig. 35. The methodology can be modified to measure the electrical resistance of the specimens during such loading. The study analyzes the structural damage observed during testing in great detail, providing deeper understanding of microscopic fractures and micro-buckling mechanism.

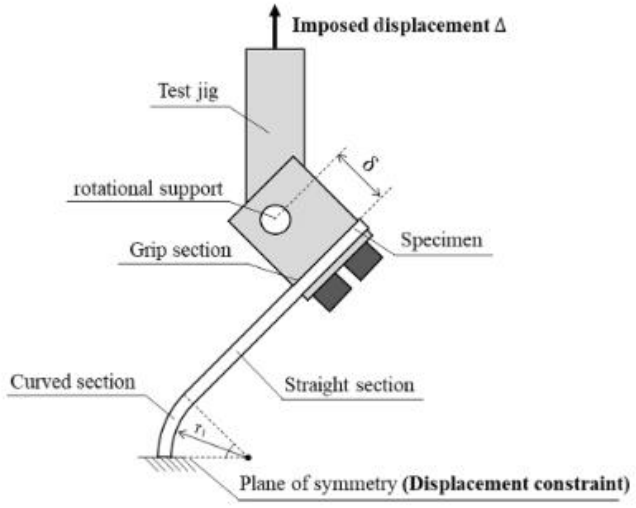

Fig. 35. Scheme of designed jig and the constraint condition for the FEM analysis [23]

3D printing of continuous carbon fiber reinforced polymers requires some pre-processing of the continuous carbon fiber strands. Such process is described in research by Rimašauskas [24] it shows the process of continuous carbon fiber strand impregnation. Fig. 36. shows the process diagram for carbon fiber strand impregnation, where (1) is the spool with impregnated carbon fiber, (2) – impregnated carbon fiber strand, (3,4) – identical diameter heating nozzle, (5) – exit nozzle of the impregnation chamber, (6) – inlet nozzle of the impregnation chamber, (7) – impregnation solution, (8) – impregnation chamber with immovably fixed roller, (9) – non-impregnated carbon fiber strand. This method creates pre-impregnated filament for use in a modified MeCreator 3D printer, which performs a secondary impregnation during printing inside the dual-inlet nozzle. This method ensures that the inside of the carbon fiber strand had better interface contact between the matrix and the carbon fiber strand.

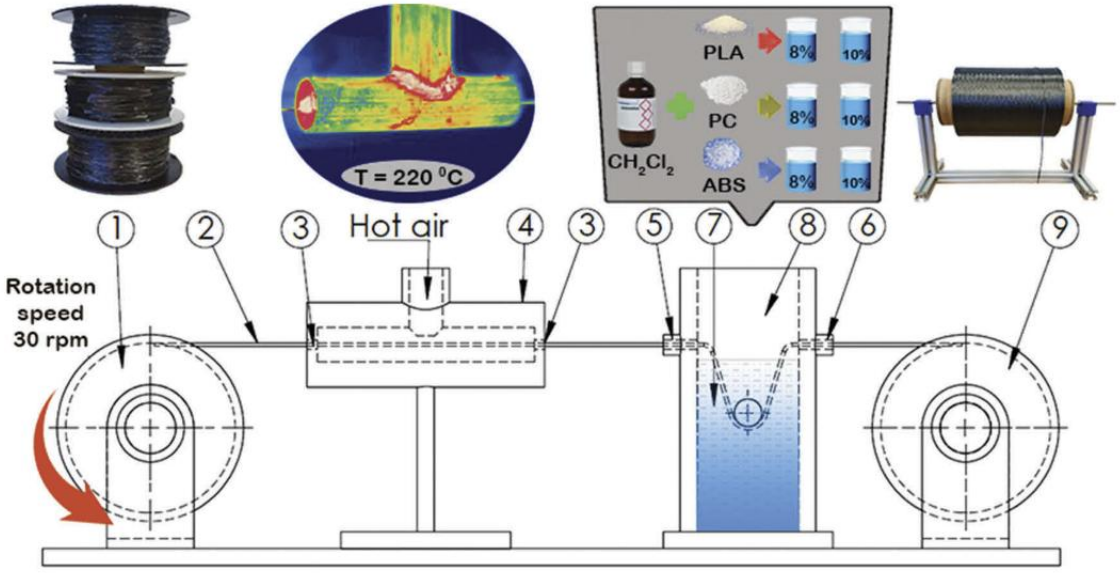

Fig. 36. Scheme for carbon fiber impregnation [24]

The chosen methodology to conduct the loading experiments on 3D printed specimens is cantilever beam due to its convenience to change the test specimens and small fixture size to enable the tests to be conducted inside the thermal chamber. The loading method chosen is an electromagnet with neodymium magnets glued to the specimens due to the ability to easily control the load and small size of the electromagnet.

2.1. Chapter summary

Overall, this chapter analyzes various research studies, the testing and manufacturing methodologies described in them. From using multiple nozzles to insert continuous carbon fiber strand into the 3D printed specimens, to pre-impregnated carbon fiber strands to achieve better matrix-fiber boundary adhesion. Also, multiple testing methodologies for loading and measuring the specimens are described. From bending tests, such as, three-point bending test and cantilever beam test, to Resistance measurement during loading, and curved profile specimen bending test setup. The chosen methodology is a combination of cantilever beam with loading from the electromagnet.

3. Resistance measurement under dynamic and static loading

The test specimens were 3D printed using a modified FDM 3D printer, where the nozzle was modified to accept two input feeds. PLA filament was fed into the first input feed, and impregnated 3k carbon fiber strand was fed into the second feed. Inside the nozzle the carbon fiber strand is coated with melted PLA filament and is extruded through the nozzle. The printed specimens were processed after printing by filing down the contact points to reach bear carbon fiber strands and gluing a conductive copper tape of 0.055 mm thickness. 0.07 mm^2 wires were soldered to the copper contact patches. A schematic drawing of the printer nozzle is shown in Fig. 37. [25]

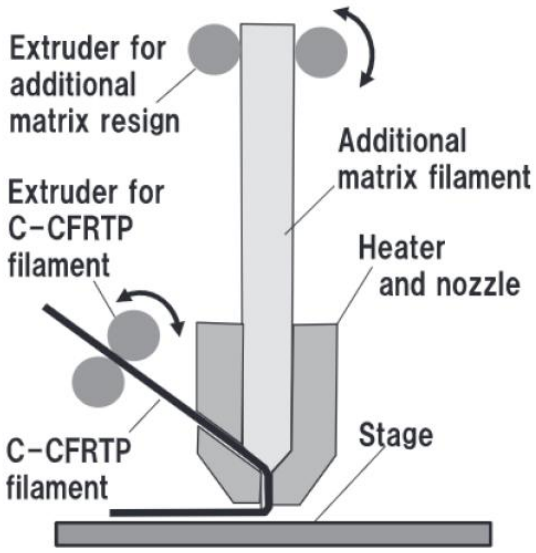

Fig. 37. Schematic of the 3D printer head used to print test specimens [25]

Testing methodology was developed to cyclically load the test specimens and record the change in electrical resistance. To cyclically load the specimen a magnet (Fig. 38. A) was glued to the specimens (Fig. 38. B). A fixture (Fig. 38. C) was made to clamp a specimen in cantilever beam configuration. A KK-P40/20 electromagnet [26] (Fig. 38. D) is used to apply a magnetic field to the specimen. The resistance measurement is taken at contact points of the specimen (Fig. 38. E). The clamps in the fixture were insulated using insulating Kapton tape.

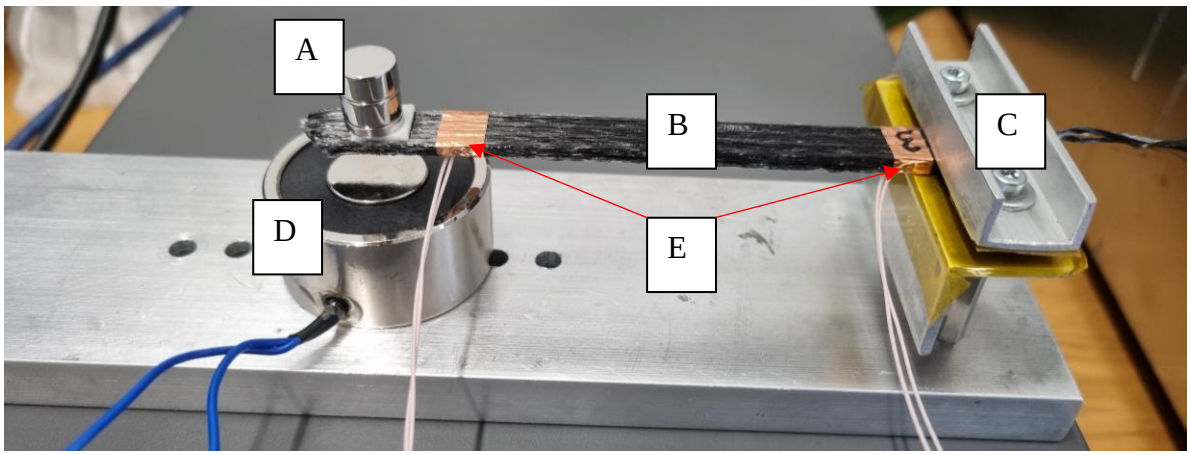

Fig. 38. Testing fixture: A – magnet, B – test specimen, C – fixture, D – electromagnet, E – measurement contact points

Moreover, the measurement setup is shown in Fig. 39. A waveform for electromagnet activation is generated using a Rigol DG1032Z arbitrary waveform generator [27] (Fig. 39. 2). The signal is amplified to reach activation voltage of the electromagnet using MMF LV 102 power amplifier [28] (Fig. 39. 3). The output voltage is measured using Fluke 289 TRMS multimeter [29] (Fig. 39. 4). The amplified signal is sent to the electromagnet, which attracts the magnet on the specimen cyclically. Electrical resistance is measured using Keithley 2614B source measure unit [30] (Fig. 39. 5) by loading a script from the computer (Fig. 39. 6) to the unit and exporting the results to a USB drive. The results file is then processed on the computer. The result files are formatted, and x-y scatter graphs are created.

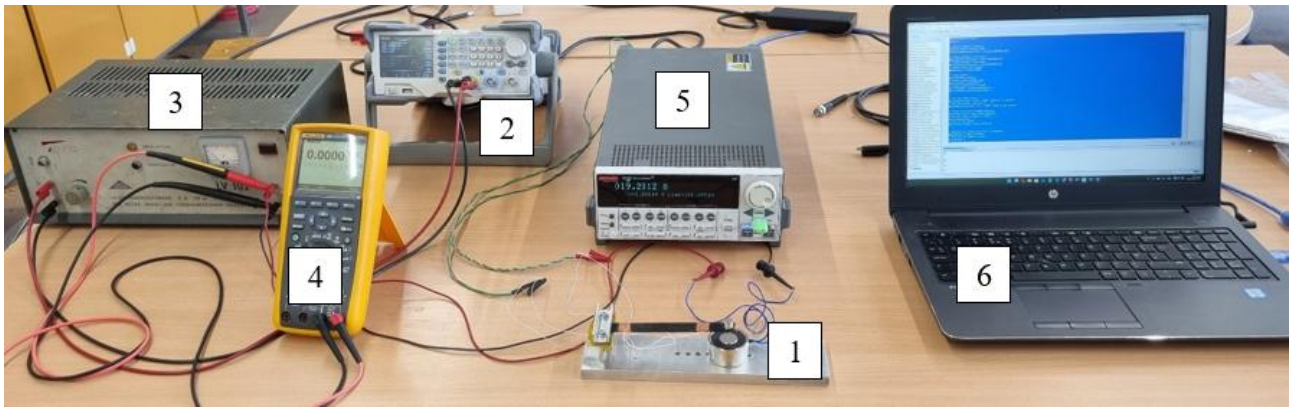

Fig. 39. Testing setup: 1 – testing fixture, 2 – Rigol DG1032Z arbitrary waveform generator, 3 – MMF LV 102 amplifier, 4 – Fluke 289 TRMS multimeter, 5 – Keithley 2614B source measure unit, 6 – computer

Furthermore, small changes in the environment, such as temperature fluctuations and people moving around caused unreliable measurement results, thus the testing fixture was placed into a Memmert UNB 400 unversal oven [31], shown in Fig. 40., set to 25°C. The testing fixture placed in the oven is shown in Fig, 41.

Fig. 40. Memmert UNB 400 universal oven

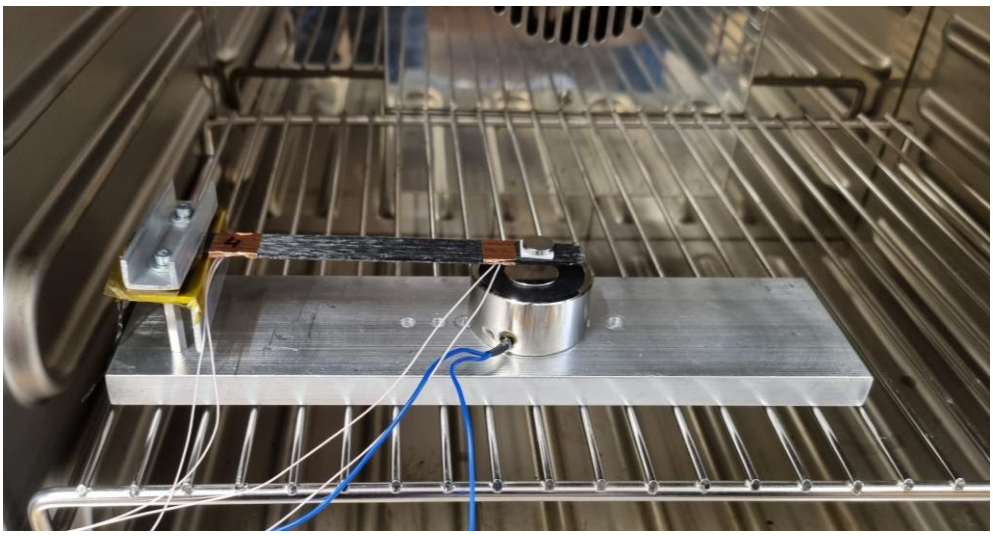

Fig. 41. Testing fixture placed inside the Memmert UNB 400 universal oven

Cyclical loading testing was done by setting the Rigol DG1032Z arbitrary waveform generator to a sinus wave with 1Hz frequency and 3V (rms) amplitude, shown in Fig. 42. The signal was amplified to 30 V peak-to-peak using the MMF LV 102 power amplifier.

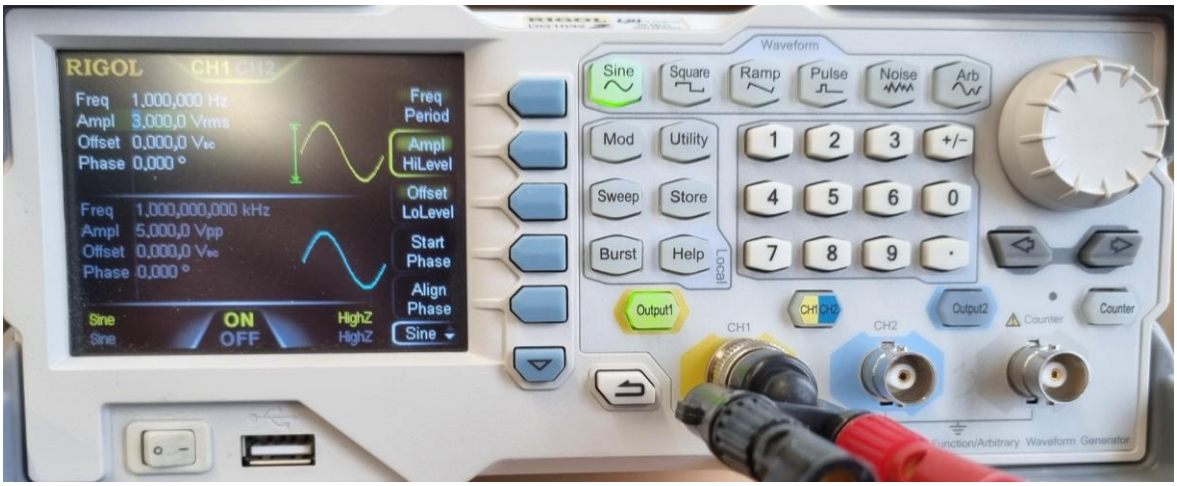

Fig. 42. Rigol DG1032Z arbitrary waveform generator settings

The Keithley 26114B source measure unit was programmed using a script shown in Appendix 1.

3.1. Experiments

Two tests were conducted for each specimen. The first test was performed during cyclical loading of the specimen, the second test was done without loading the specimen over a longer period of time to determine the internal electrical resistance of the specimens. The number of magnets is varied between specimens due to their stiffness to reach 5mm displacement amplitude at the end of the specimen.

During the first test measurements were taken every 0.05 s for 7200 measurements. The tests were conducted inside the universal oven to reduce the effect of environment changes on the specimens. During the second test the measurements were taken every second for 1800 measurements. The specimens were left at rest to measure their internal resistance.

3.1.1. First test specimen

The first specimen (Fig. 43.) was tested using one 1mm thick and one 3mm thick neodymium magnets of 10mm diameter. The specimen dimensions are: 138 mm length, 13 mm width, and 2.5 mm thickness.

Fig. 43. First test specimen

The first test results are shown in Fig. 44. The results show an increase of resistance over time while cyclically loading the specimen, this may be caused by increase in temperature while loading the specimen. The shorter time interval results show clear periodical resistance from 26.41808 Ω when loading is inactive and increases to 28.97922 Ω when the electromagnet is activated. The fluctuations on the lower part of the graph show the rebound of the test specimen when loading is inactivated.

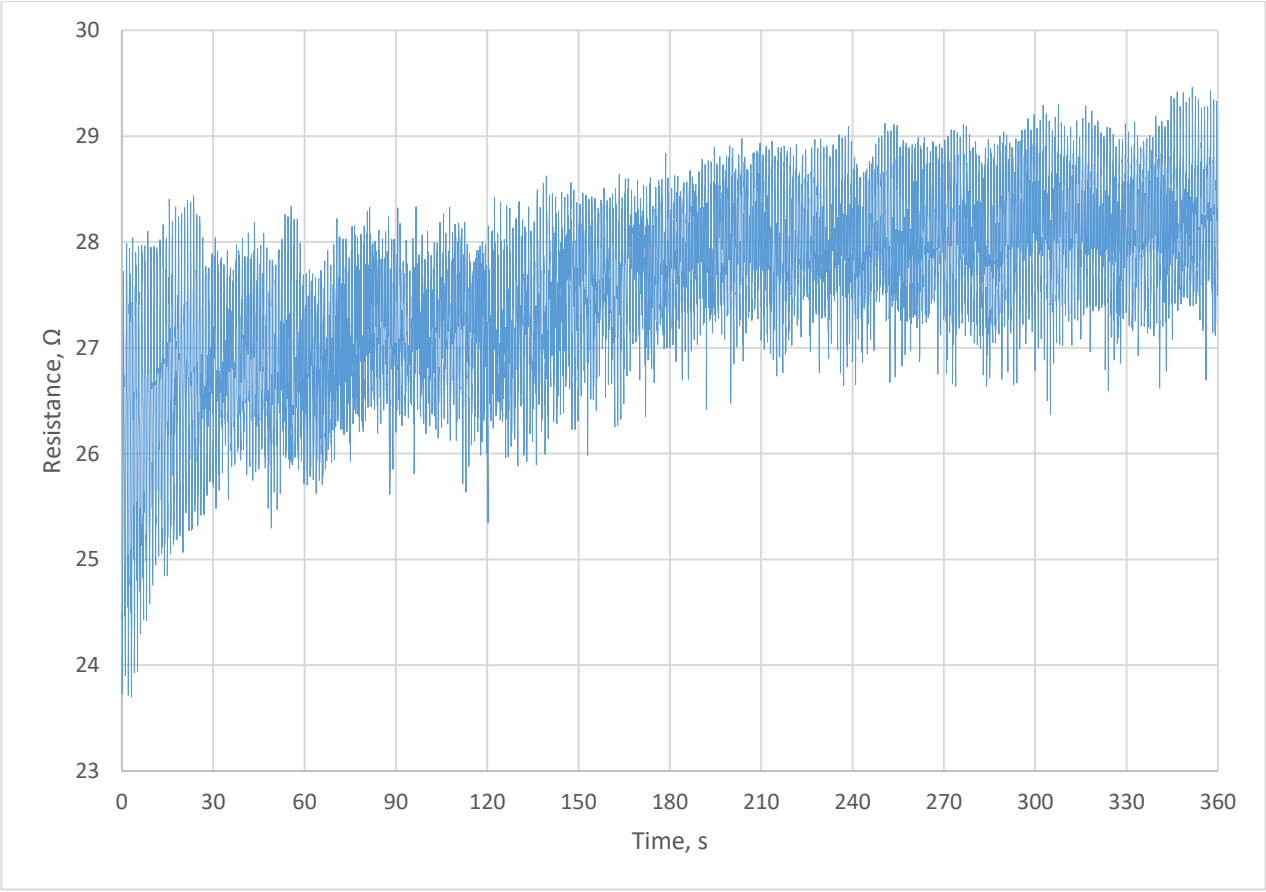

Fig. 44. Results of first test for the first specimen

Shorter time interval results are shown in Fig. 45.

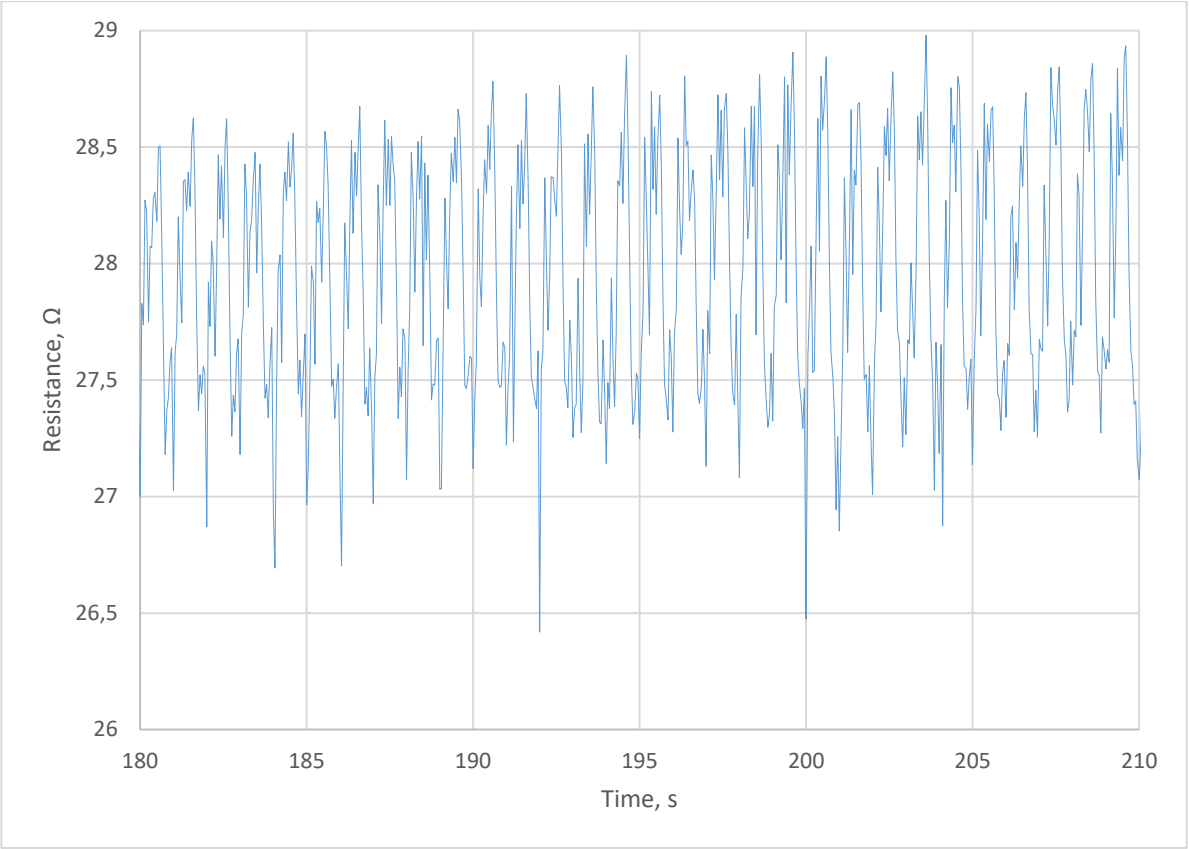

Fig. 45. Short interval test results of the first test for the first specimen

The results of the second test are shown in Fig. 46. The results show that the resistance settles over time to 20.16899 **Ω** average after 500 seconds. This may be caused by the measurement equipment applying small voltage to measure resistance, this may cause the carbon fiber strand to heat up, thus increasing the resistance. The resistance settles because the fibers reach equilibrium over time and the resistance decreases.

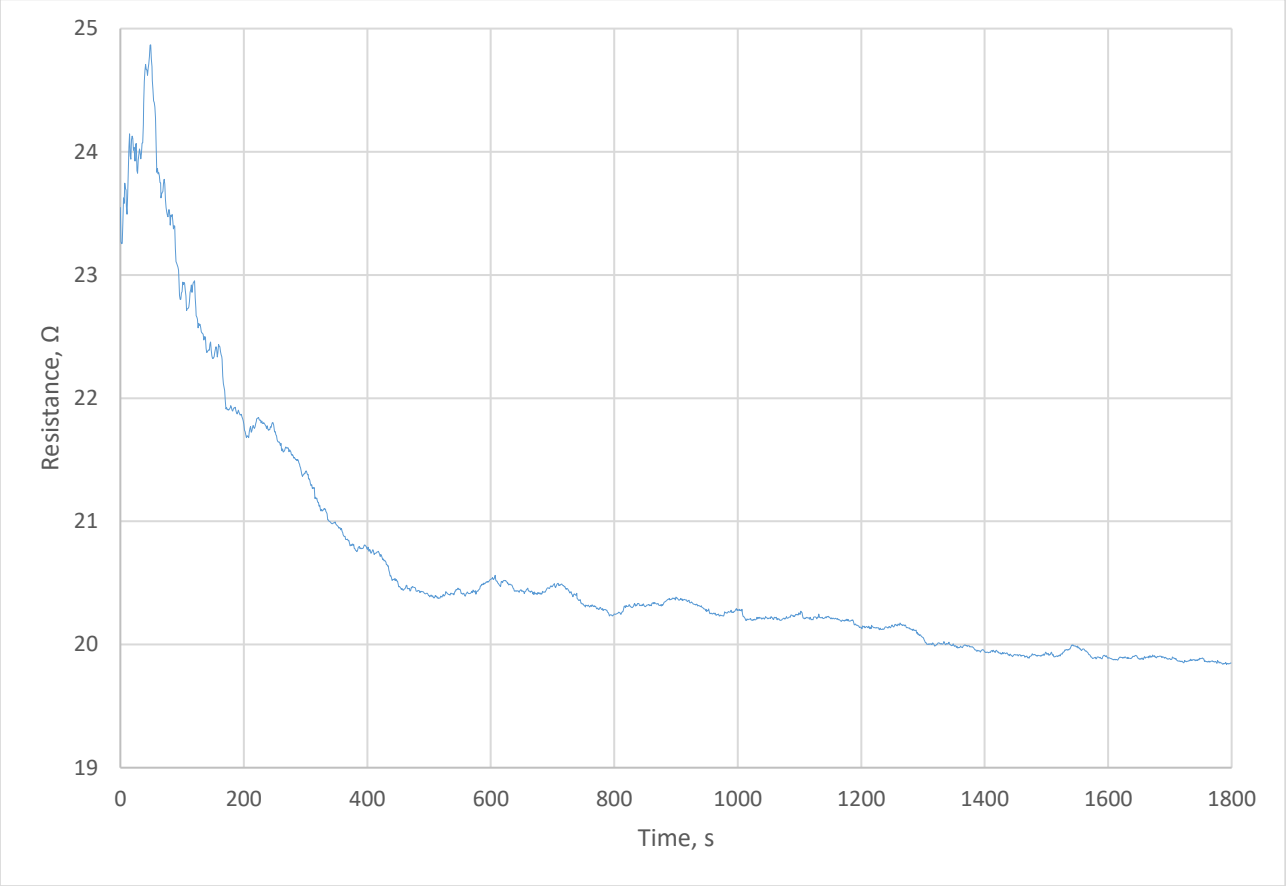

Fig. 46. Results of the second test for the first specimen.

3.1.2. Second test specimen

The second specimen (Fig. 47.) was tested using an M6 nylon-locking nut instead of a magnet, because the stiffness of the specimen was too low to support a magnet without it attracting the inactivated electromagnet. The specimen dimensions are: 121 mm length, 16.5 mm width, and 1.3 mm thickness.

Fig. 47. Second test specimen

The results of the first test are shown in Fig. 48. The results show that the resistance decreases over time during the loading cycle. The second test specimen is thinnest of all test specimens, this may cause the resistance to decrease due to its flexibility. The specimen is able to dissipate heat more rapidly than other specimens and heat is more rapidly distributed throughout the specimen. The shorter time interval results show clear periodical resistance fluctuations between 14.31251 Ω and 14.74599 Ω.

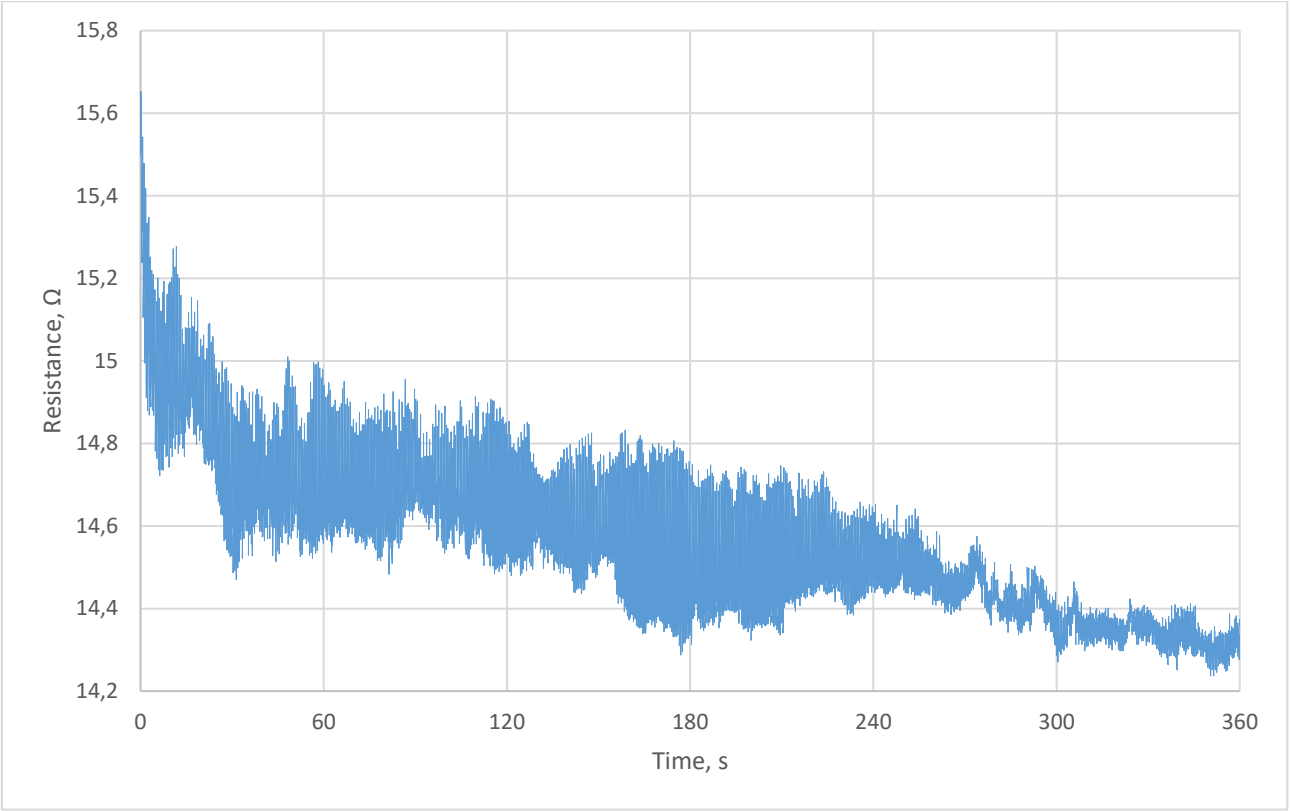

Fig. 48. Results of the first test for the second specimen

Shorter time interval results are shown in Fig. 49.

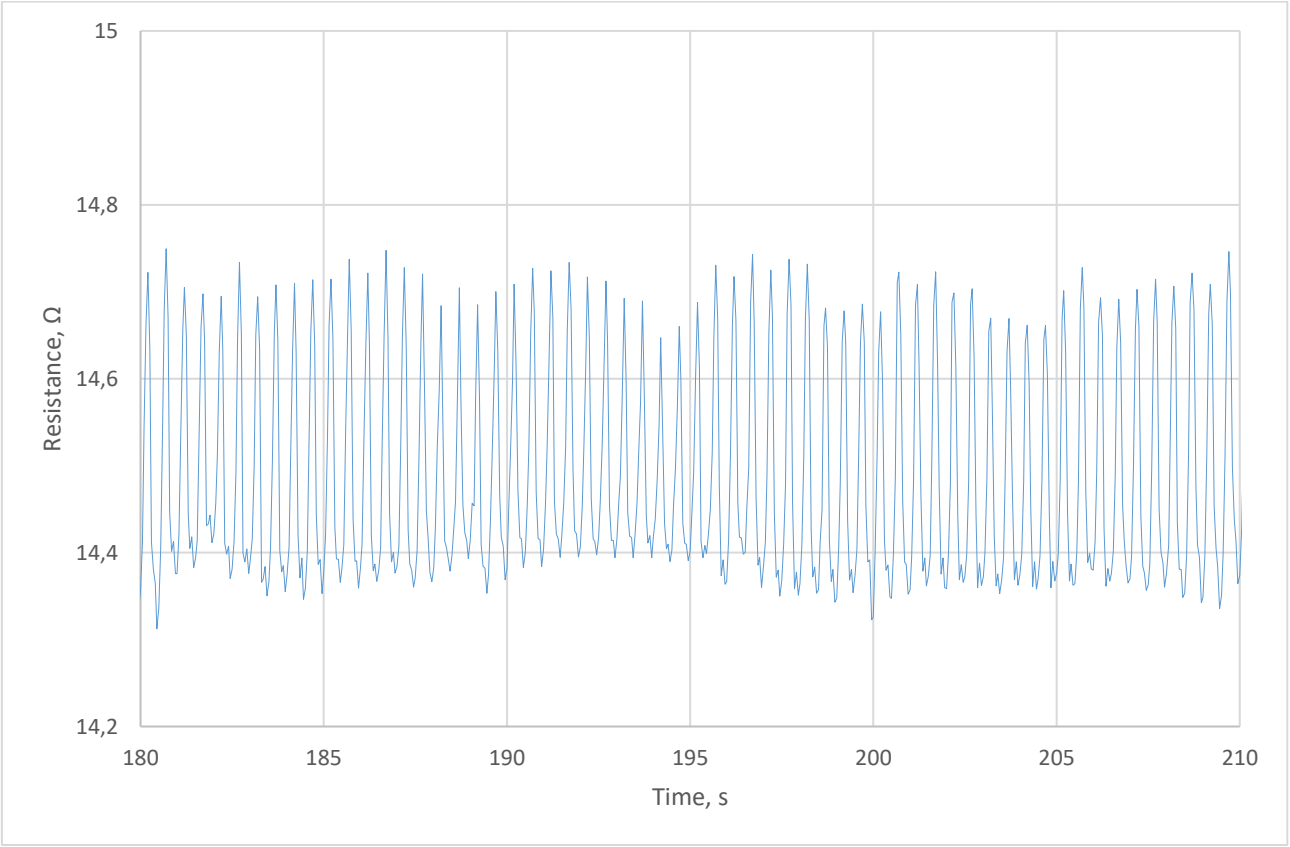

Fig. 49. Short interval test results of the first test for the second specimen

The results of the second test are shown in Fig. 50. Similar to the first specimen the resistance value settles over time to 14.39236 Ω average after 700 seconds due to the applied voltage for measurement of resistance.

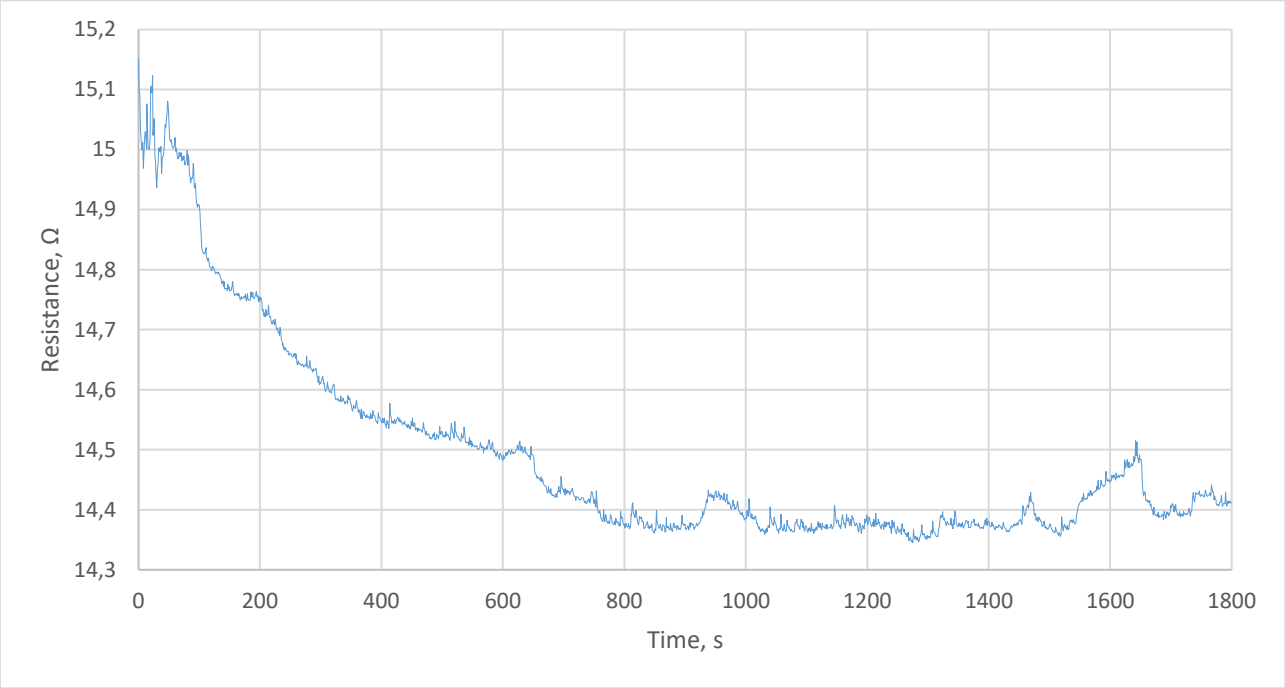

Fig. 50. Results of the second test for the second specimen

3.1.3. Third test specimen

The third specimen (Fig. 51.) was tested using one 1mm thick and one 3mm thick neodymium magnets of 10mm diameter. The specimen dimensions are: 131 mm length, 10.5 mm width, and 3.5 mm thickness.

Fig. 51. Third test specimen

The results of the first test are shown in Fig. 52. The results show a fluctuation of resistance over time, this may be caused by the stiffness of the specimen. It is the thickest of all test specimens, therefore, the time needed to dissipate the heat is higher than other specimens. The value settles after 240 seconds. The shorter time interval results show clear periodical change in resistance from 27.77428 Ω to 31.95276 Ω with the highest variability of all the specimens due to its stiffness. Also, the rebound effect when the electromagnet is deactivated is the highest of all the specimens.

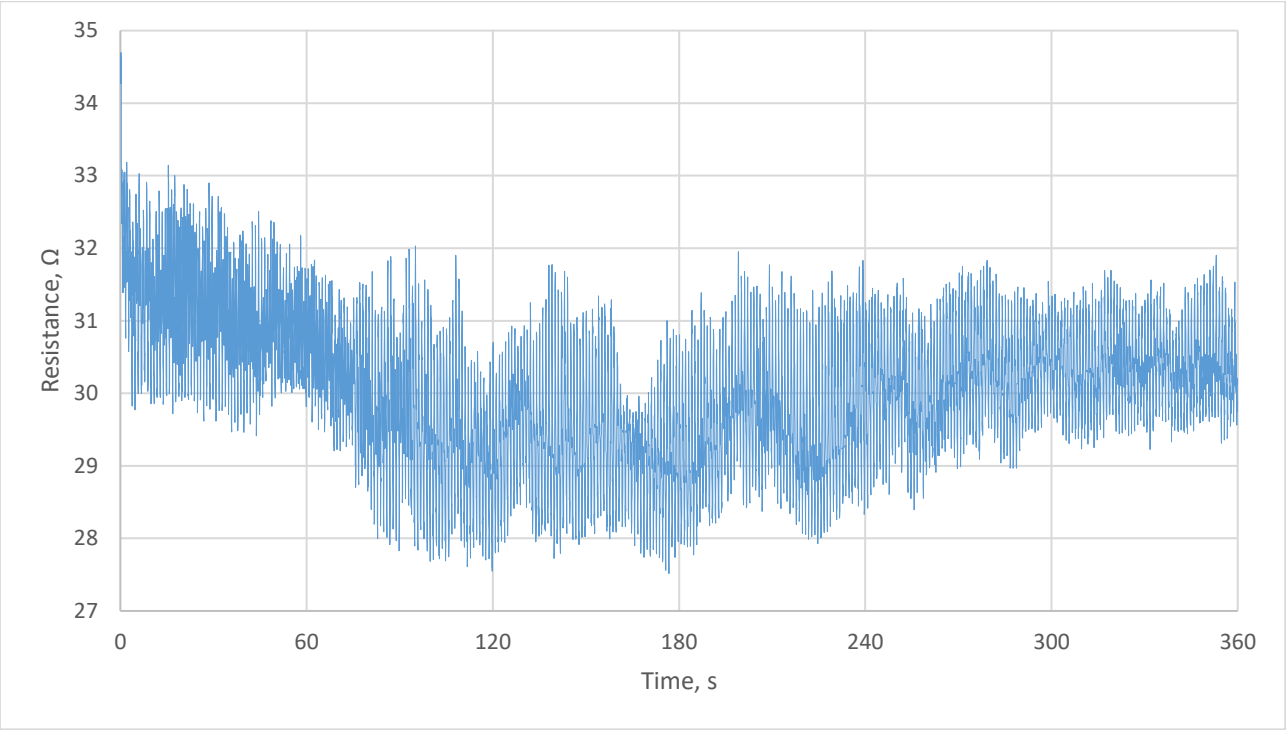

Fig. 52. Results of the first test for the third specimen

Shorter time interval results are shown in Fig. 53.

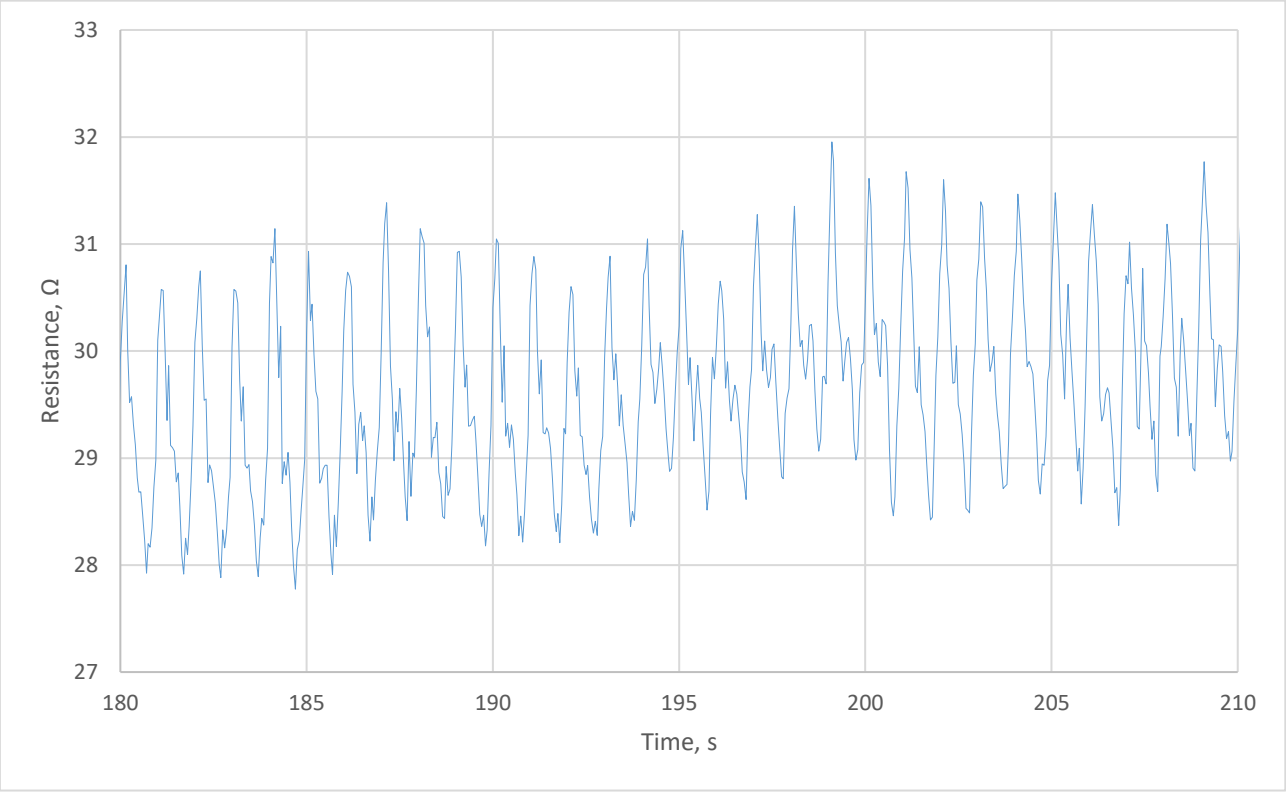

Fig. 53. Short interval test results of the first test for the third specimen

The results for the second test are shown in Fig. 54. The results show that the change in resistance value is the lowest from all the specimens, this is due to the stiffness of the specimen. The specimen

stiffness improves stability, thus reducing the change in resistance. The resistance settles to 26.15191 Ω average resistance after 200 seconds.

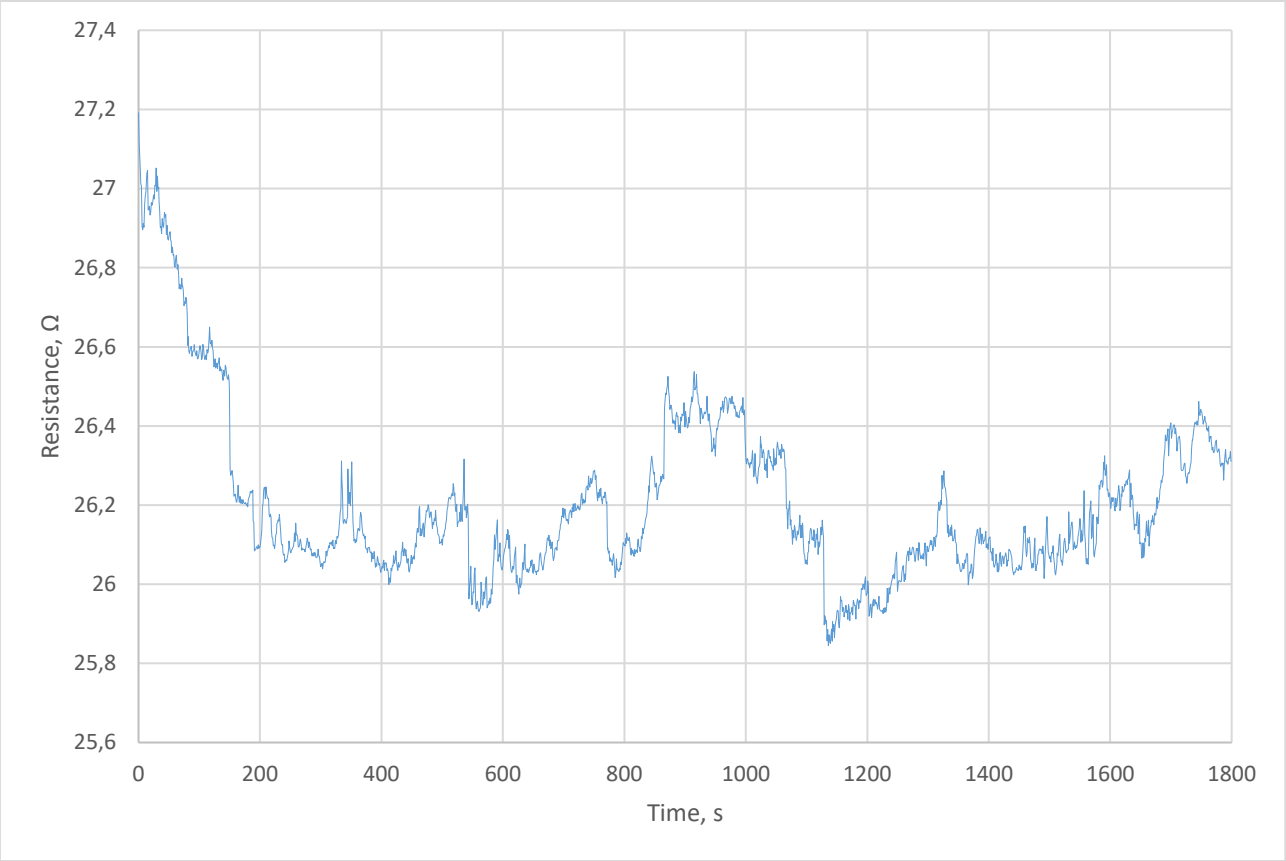

Fig. 54. Results of the second test for the third specimen

3.1.4. Fourth test specimen

The fourth specimen (Fig. 55.) was tested using one 1mm thick and two 3mm thick neodymium magnets of 10mm diameter. The specimen dimensions are: 144 mm length, 13 mm width, and 2 mm thickness.

Fig. 55. Fourth test specimen

The results of the first test are shown in Fig. 56. Similar to the first specimen the results show an increase in resistance over time. This is caused by the increase in temperature inside the specimen. Shorter time interval results show periodical change in resistance from 18.07851 Ω to 20.57792 Ω.

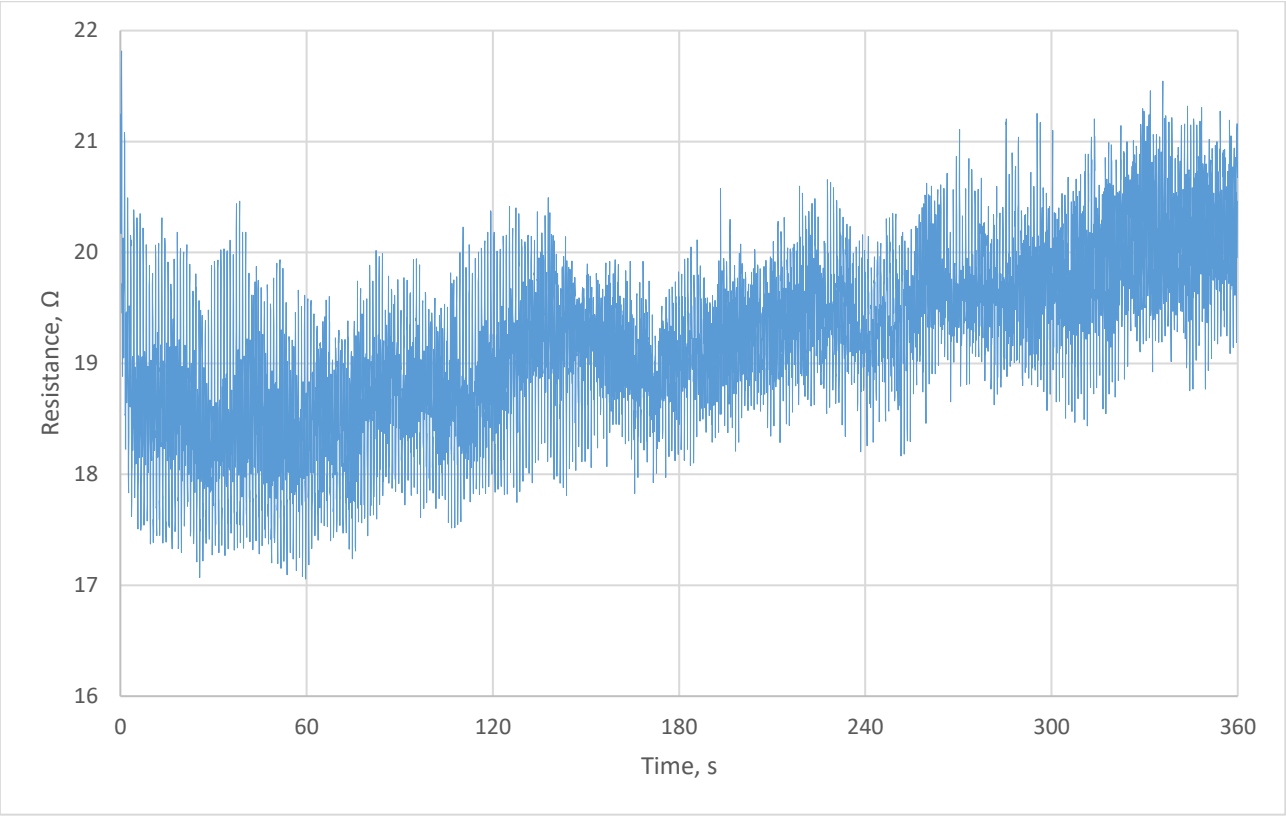

Fig. 56. Results of the first test for the fourth specimen

Shorter time interval results are shown in Fig. 57.

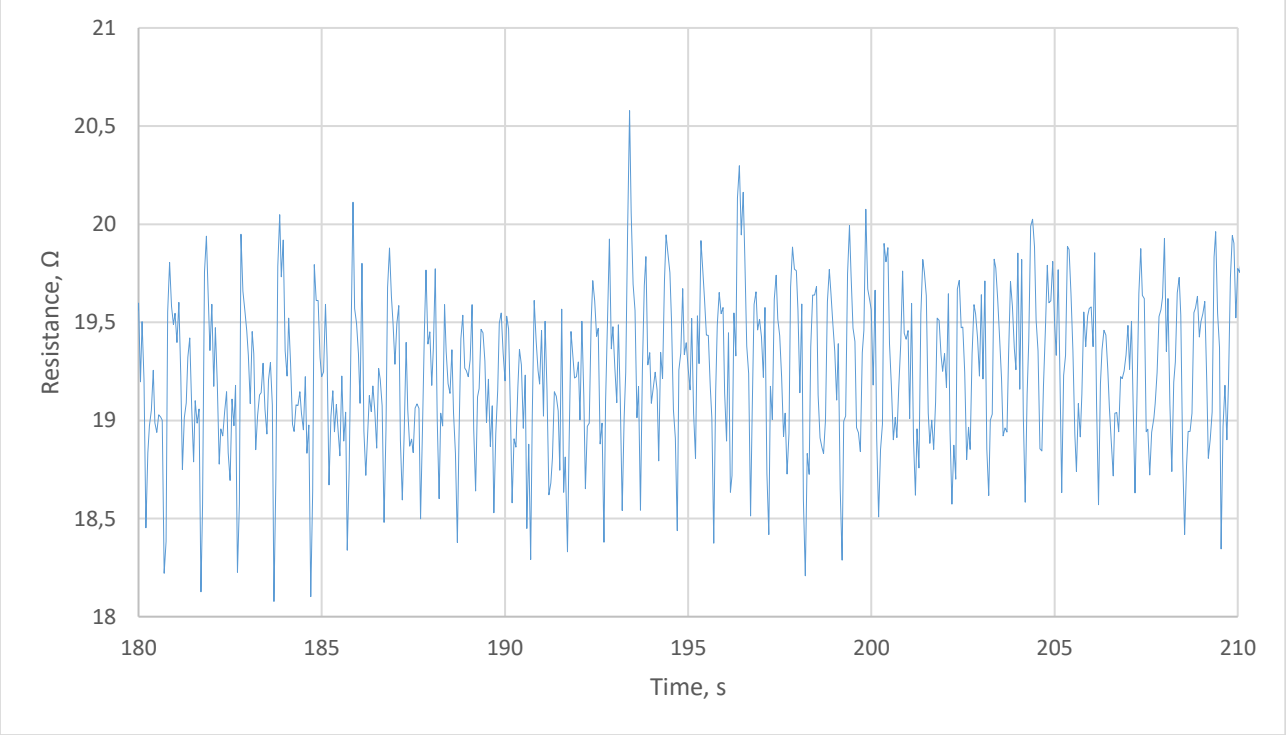

Fig. 57. Short interval test results of the first test for the fourth specimen

The results of the second test are shown in Fig. 58. The results show that the resistance settles over time to 14.79268 Ω average after 600 seconds.

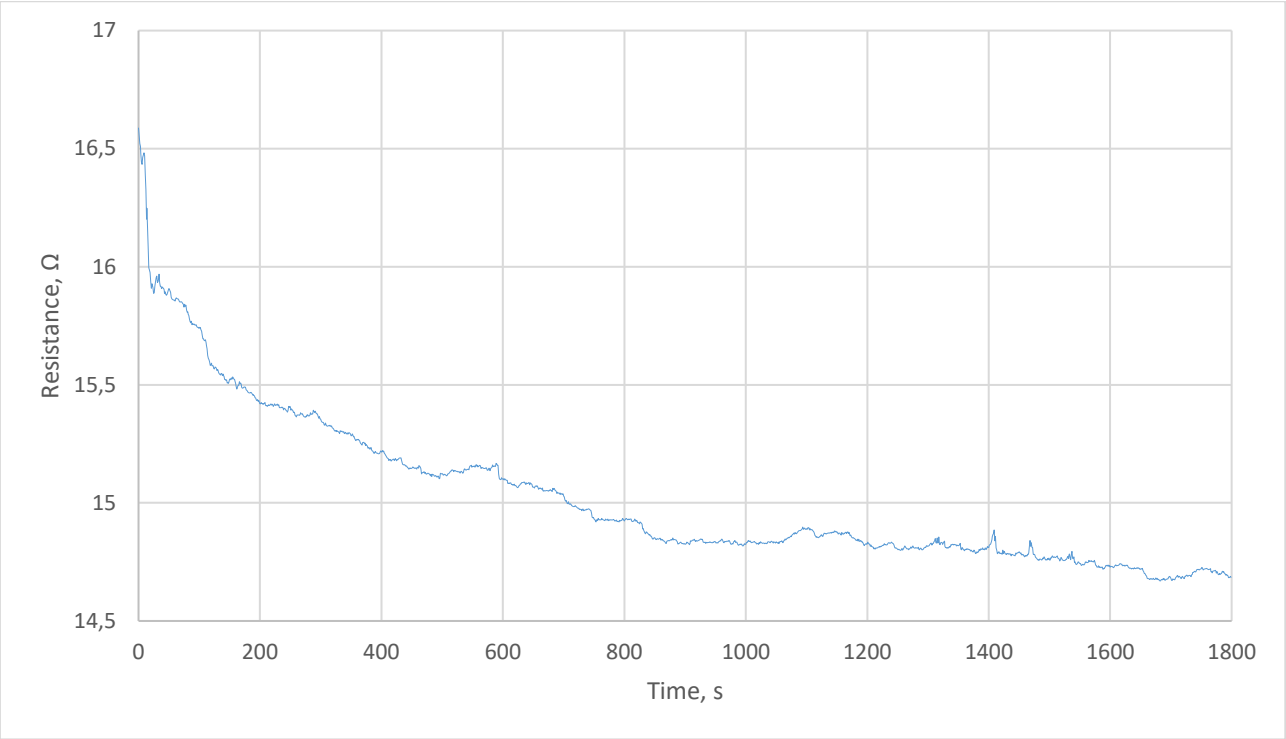

Fig. 58. Results of the second test for the fourth specimen

3.2. Comparison of the test results for all specimens

Combined results of test No. 1 for all specimens are shown in Fig. 59. The results show that the resistance values for each specimen vary from 14.2367 Ω in specimen No. 2 to 34.69753 Ω in specimen No. 3. This shows that if a load sensor is designed using piezoresistive properties of continuous carbon fiber strand each specimen should be tested and the values recorded to provide the baseline readings for sensor application. The measured resistance depends on the specimen stiffness and carbon fiber content in the specimen.

Fig. 60. shows a shorter time interval of the test No. 1. The results show a sinusoidal change in resistance in all specimens, thus proving that CCFRP composites can be used as sensors.

Also, combined results of test No. 2 are shown in Fig. 61. The results show that the resting resistance values for each specimen vary from 14.49185 Ω in specimen No. 2, to 26.20589 Ω in specimen No. 3. This shows that the stiffness of the specimen, as well as, carbon fiber content has influence on the initial resistance of the specimen. The stiffness does not influence it directly, however, during testing the variability of the measurements was greater in higher stiffness specimens. The initial increase in resistance can be seen in all the specimens due to the voltage applied during measurement, it gradually decreases over time and settles to a relatively steady resistance reading.

The tested specimens differ in their volume, thus requiring different amounts of 3D printing filament, therefore, the carbon fiber content depends on the filament amount. The highest carbon fiber content specimen is the stiffest, because of the carbon fiber reinforcement. The carbon fiber content has dual purposes in this kind of sensor. The higher the carbon fiber content the harder it is to deform, but the load measurement capacity of the sensor increases as well.

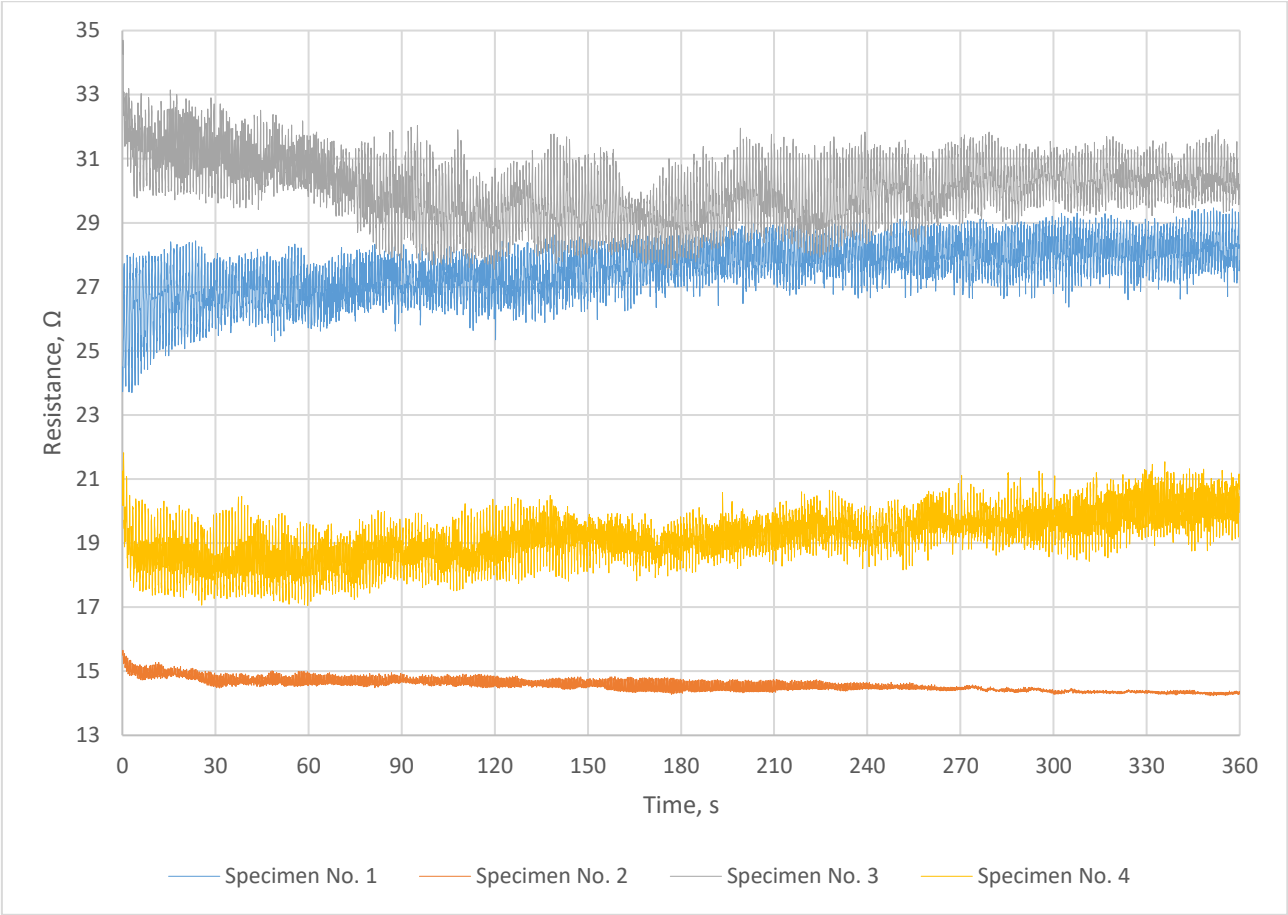

Fig. 59. Combined results of test No. 1 for all specimens

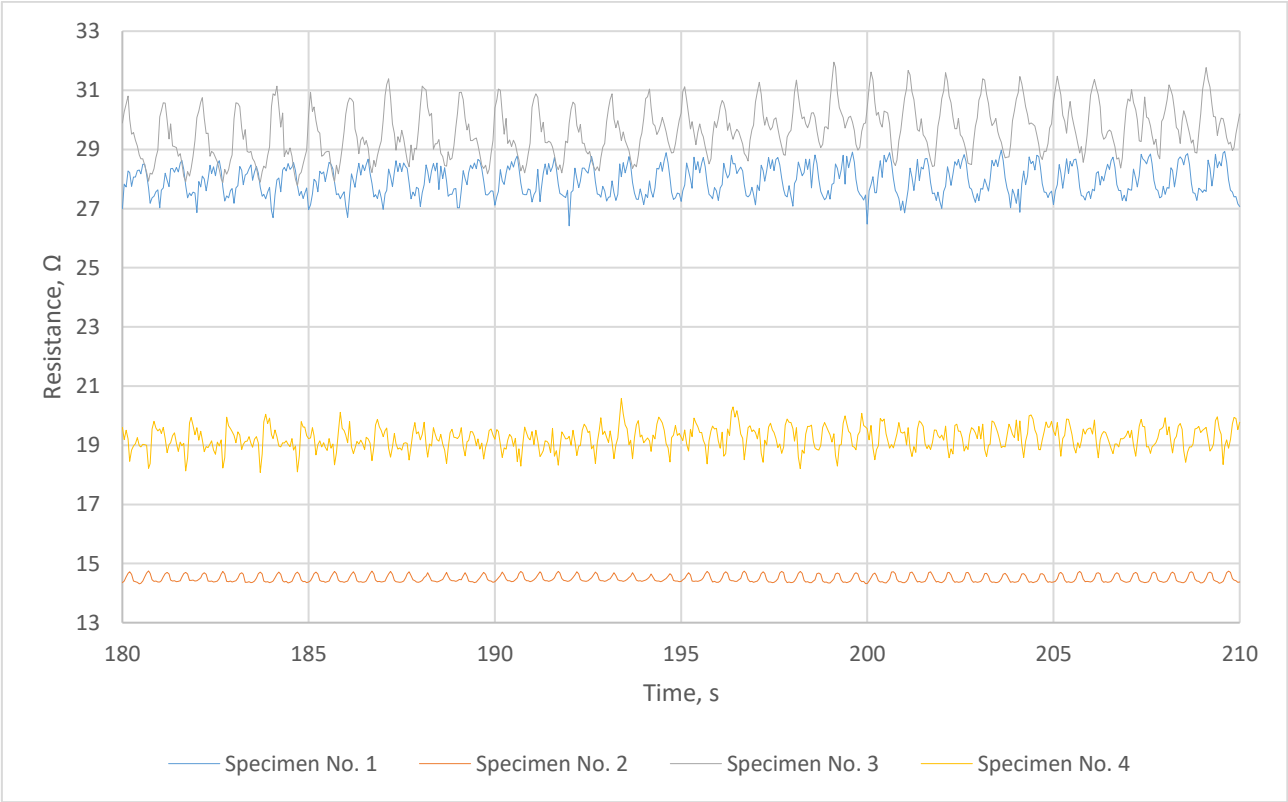

Fig. 60. Combined results of test No. 1 shorter time interval for all specimens

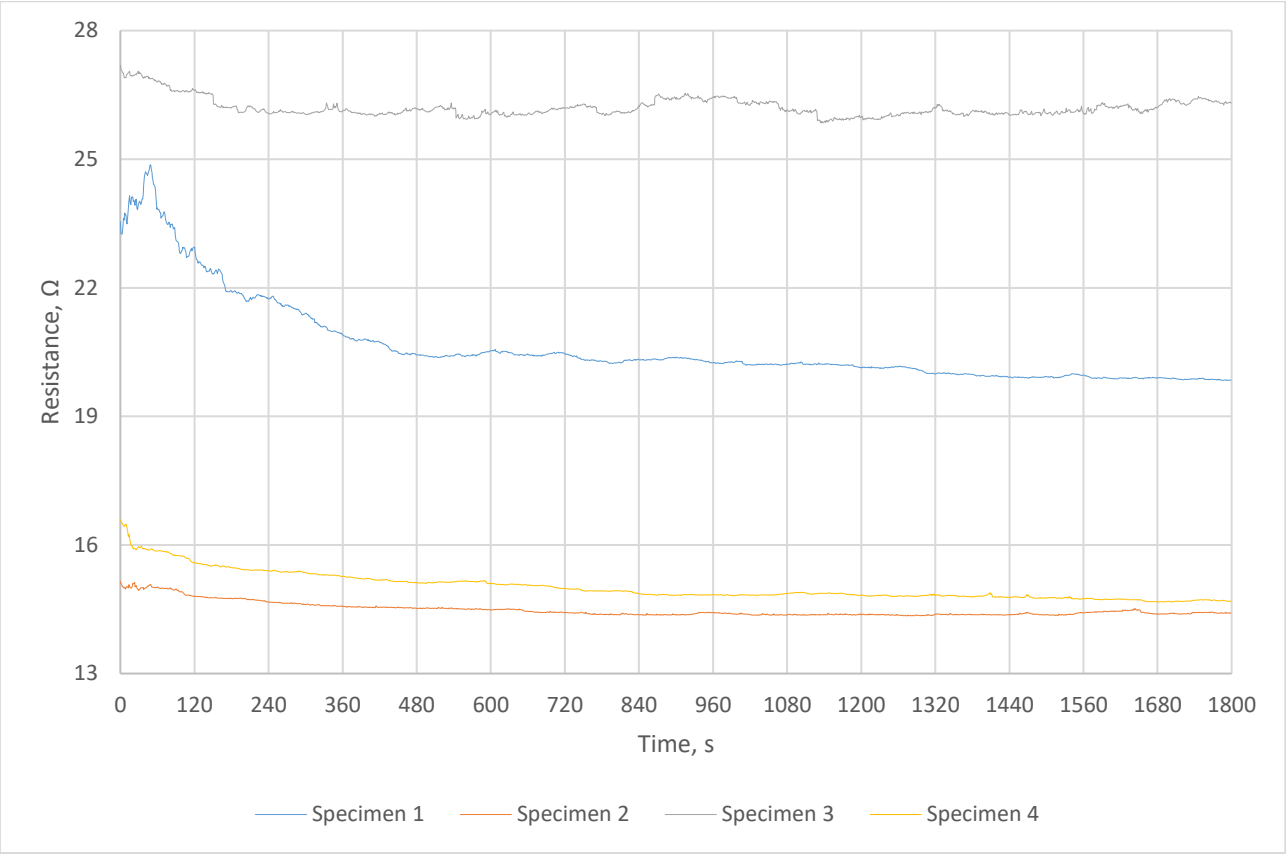

Fig. 61. Combined results of test No. 2 for all specimens

3.3. Testing conclusions

During cyclical load cantilever beam bending tests continuous carbon fiber reinforced 3D printed specimen electrical resistance results show sinusoidal change. The results of the first and the fourth specimens show that the resistance increases over time, this may be caused by a number of factors such as:

- Matrix consolidation, caused by cyclical loading of the specimens, where matrix material polymer chains are reoriented and repositioned. This causes the stiffness of the specimen to increase similar to work hardening of metals.
- Microstructural changes, cyclical loading may create microstructural changes in the matrix material. Some of the changes are densification, recrystallization and cross-linking. The effects may become noticeable over time when the specimen is loaded for a longer period of time. The specimen's resistance to bending loads increases during longer loading periods.
- Creep behavior, thermoplastic matrix deforms under constant load over time, during cyclical loading the matrix undergoes creep deformation during each cycle. The accumulated creep deformation of the matrix may cause the increased resistance to bending, thus causing higher electrical resistance.
- Fiber reorientation, continuous carbon fibers may reorient fibers on microscopic scale during loading to resist the load applied. This may cause the resistance to increase due to changes in fiber orientation.

The second and the third specimens show decrease in resistance over the testing period. This may be caused by:

- Micromovements of the contact patch between the contact pads and the specimen fibers. During cyclical loading the contact patch moves, thus causing a change in electrical resistance of the specimen. The contact pad may have a better conductivity when more of the internal fibers are touching the contact pad.
- Fatigue damage to the carbon fibers. The fibers may have experienced microscopic fatigue fractures, thus changing the electrical resistance, if more of the fibers are touching each other the resistance may be decreased.

The resting resistance of all specimens show that the specimens need time to settle when measuring their electrical resistance. This may be caused by the current passed through the specimens during measuring. The continuous carbon fibers heat up when the current is applied, when the temperature reaches equilibrium the resistance values settle. The unloaded specimens should be measured for a longer period of time to calibrate the resistance change during loading if used in 3D printed parts.

Table 1. shows the results from conducted experiments. The volume is calculated from specimen measurements, change in resistance is calculated from the shorter time interval graphs to eliminate initial rise in electrical resistance. Initial resistance value is the average resistance when testing without load and removing initial rise in resistance.

Table 1. Dynamic loading test results for all specimens

	Specimen No. 1	Specimen No. 2	Specimen No. 3	Specimen No.4
V, mm^3	4485	2595.5	4814.25	3744
ΔR, Ω	2.56114	0.43348	4.17848	2.49941
R_0, Ω	20.63464	14.49185	26.20586	15.02602

The second specimen results showed the lowest electrical resistance values due to the shortest length of the carbon fiber strand in all specimens. Also, it showed the highest precision with change in resistance of 0.43348 Ω and initial resistance of 14.49185 Ω. In some industries, such as, aerospace, biomedical or sports a high precision might be required. The test results show that a thinner sensor should be produced to increase its accuracy and sensitivity to the change of load.

The third specimen results showed the highest resistance values due to the longest length of carbon fiber strand in the specimen. Also, it showed the lowest precision with change in resistance of 4.17848 Ω and highest initial resistance of 26.20586 Ω. This shows that for industries, such as construction and others that require high strength, and high load capacity, a thicker sensor should be produced. This reduces the sensitivity and precision of the sensor, but increases the stiffness of the part.

This proves that the carbon fiber content in the specimen is directly related to the resistance values in the specimen. To improve the accuracy of the sensor a shorter length of carbon fiber strand should be used, taking into account that the strength of the part will be reduces due to the reinforcing material content being reduced.

The conducted tests show that the test specimens have sensing properties, and can be used to show loading data over time. The continuous carbon fiber reinforced polymer parts can be used as sensors for mechanical loads.

3.4. Chapter summary

The tests were conducted inside the oven to prevent environmental effects. The specimens were placed on the testing jig for cantilever beam bending tests, and the loading was applied using an electromagnet and neodymium magnets glued to the specimens. Two tests were conducted for each specimen, the first one with 1 Hz frequency 5mm amplitude cyclical loading, the second one without the loading. The test results were processed into graphs. The results showed that 3D printed CCFRP composited can be used as mechanical load sensors.

4. Economic evaluation of 3D printed CCFRP sensors

3D printed CCFRP sensors excel at the ability to be customized, thus the cost comparison between custom made traditional load-cell based sensor and 3D printed sensor was conducted.

According to Meena [32] a typical load-cell based sensor development and manufacturing costs from 5000 € to 50000 € depending on the complexity of the sensor and customized properties. Average cost being 25000 €. One unit is usually sold from 300 € to 3000 €, taking average price of 1350 €

Taking into account the average hourly wage of a mechanical engineer in Lithuania of 10 €/h [33].
The average electricity cost per kWh of 0.24 € [34].
The average design time for a specific part of 40 hours.
Taking average printing time of 12 hours.
Testing time was taken from the testing procedure of this project of 7 hours.
Taking that the 3D printed CCFRP sensor would be integrated into a part of 200 mm by 200 mm by 50 mm, and the sensing part is 100 mm by 5 mm by 2 mm.

The filament mass needed to print such part with 100% infill:

$m = V \cdot \rho$;

$200\ mm \cdot 200\ mm \cdot 50\ mm \cdot 1.25 \frac{g}{mm^3} = 2500\ g$;

Average price of 1 kg of PLA filament is 20 € [35]:

$Cost = mass \cdot cost\ per\ gram$;

$2500\ g \cdot 0.02 \frac{€}{g} = 50\ €$;

The required amount of 3k carbon fiber for the infill:

$V = a \cdot b \cdot h$;

$100\ mm \cdot 5\ mm \cdot 2\ mm = 1000\ mm^3$;

Taking average price for 3k carbon fiber per mm^3 is 0.0052 € [36].

$Cost = V \cdot cost\ per\ mm^3$;

$1000\ mm^3 \cdot 0.0052 \frac{€}{mm^3} = 5.20\ €$;

3D printing hourly rate is taken as 20 €/h:

$Costs = time \cdot hourly\ rate$;

$12\ h \cdot 20 \frac{€}{h} = 240\ €$;

Electricity usage of an average 3D printer is around 200 W [37]:

$Cost = electricity\ price \cdot power \cdot time$;

$0.24 \frac{€}{kWh} \cdot 0.2\ kW \cdot 12\ h = 0.58\ €$;

The labor costs for development and testing are calculated:

$Salary = \ time \cdot hourly\ wage$;

$(40\ h + 7\ h) \cdot 10 \frac{€}{h} = 470\ €$;

The development and manufacturing cost of 3D printed CCFRP sensor is calculated:

$470\ € + 0.58\ € + 240\ € + 5.20\ € + 50\ € = 765.78\ €$.

According to the calculation the average cost for developing a 3D printed CCFRP load sensor is 758.78 € in Lithuania. Compared to the average development and manufacturing cost of traditional sensor of 26350 € the 3D printed sensor is the more cost-effective option when customized sensor is required, however the cost of mass produces traditional sensor will decrease significantly over time.

Fig. 62. shows how the costs of developing and manufacturing a single unit of 3D printed CCFRP sensor are distributed.

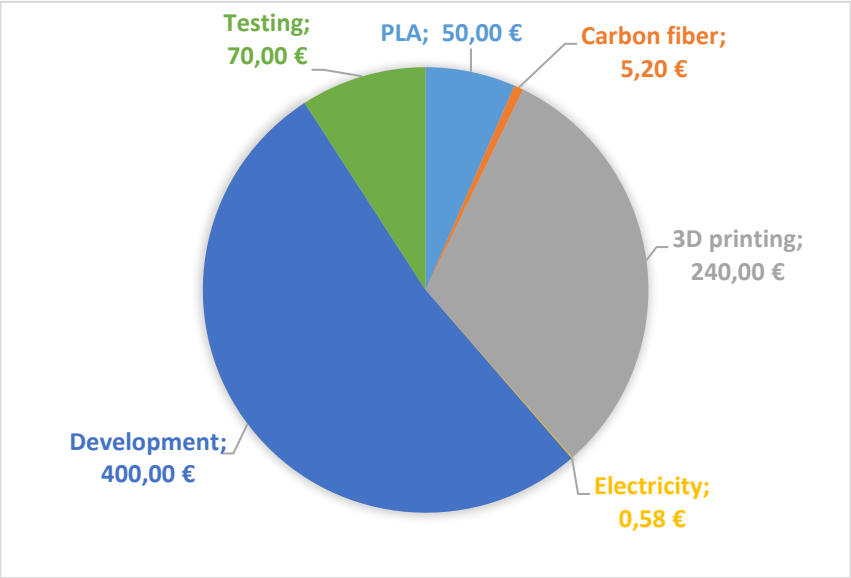

Fig. 62. Cost distribution of 3D printed CCFRP sensor development and manufacturing.

4.1. Chapter summary

Economic evaluation was done to compare traditional load-cell based sensors and 3D printed CCFRP sensors. Their development and manufacturing costs were evaluated. The evaluation showed that creating a customized load sensor is more cost-effective when utilizing 3D printed CCFRP composite technology, only when mass producing the traditional load sensors become more cost-effective.

Conclusions

The 3D printed CCFRP composites are suitable to be used as sensors due to their piezoresistive properties, especially when customized mechanical or geometrical properties are required.

1. Four continuous carbon fiber reinforced test specimens were printed with PLA filament matrix using a modified FDM 3D printer. The specimen volume was measured to 4485 mm^3, 2595.5 mm^3, 4814.25 mm^3 and 3744 mm^3 for specimens 1 – 4 respectively.

2. The test specimens were tested with static loading and the resistance values were measured at rest with neodymium magnet attracting the electromagnet surface. The Measured resistance showed that the applied voltage at the beginning of the tests increased the temperature of the specimens, thus increasing the electrical resistance. After the resting period the specimen resistance settled to 20.16 Ω, 14.39 Ω, 26.15 Ω and 14.79 Ω resistance for specimens 1 – 4 respectively.

3. Dynamic cyclical loading tests were conducted on test specimens and resistance measured during loading. Test results show that the resistance changed in I sine weave pattern, correlating to the applied load. The change in resistance during dynamic load testing was 2.6 Ω, 0.45 Ω, 3.2 Ω and 2.5 Ω for specimens 1 – 4 respectively.

4. The correlation between resistance values and carbon fiber content was determined. The test results showed that the specimen No. 2, with the lowest carbon fiber content, had the lowest change in resistance from all the specimens. As well as, the specimen No. 3, with the highest carbon fiber content, had the highest change in resistance.

5. Economic benefits of 3D printed CCFRP sensors were evaluated. The analysis showed that 3D printed CCFRP sensors are more cost-effective than traditional load-cell based sensors when a customized, low production volume sensor is required. However, when mass produced sensor is required, it is more cost-effective to develop and manufacture a traditional sensor.

List of References

1. YEONG, Wai Yee and GOH, Guo Dong. 3D Printing of Carbon Fiber Composite: The Future of Composite Industry? *Matter*. 3 June 2020. Vol. 2, no. 6, p. 1361–1363. DOI 10.1016/J.MATT.2020.05.010.
2. GUO, Haichang, LV, Ruicong and BAI, Shulin. Recent advances on 3D printing graphene-based composites. *Nano Materials Science*. 1 June 2019. Vol. 1, no. 2, p. 101–115. DOI 10.1016/J.NANOMS.2019.03.003.
3. WANG, Xin, JIANG, Man, ZHOU, Zuowan, GOU, Jihua and HUI, David. 3D printing of polymer matrix composites: A review and prospective. *Composites Part B: Engineering*. Online. 1 February 2017. Vol. 110, p. 442–458. [Accessed 3 May 2023]. DOI 10.1016/J.COMPOSITESB.2016.11.034.
4. ZHANG, Zhongsen, LONG, Yu, YANG, Zhe, FU, Kunkun and LI, Yan. An investigation into printing pressure of 3D printed continuous carbon fiber reinforced composites. *Composites Part A: Applied Science and Manufacturing*. Online. 1 November 2022. Vol. 162, p. 107162. [Accessed 3 May 2023]. DOI 10.1016/J.COMPOSITESA.2022.107162.
5. SHAFIGHFARD, Torkan and MIELOSZYK, Magdalena. Experimental and numerical study of the additively manufactured carbon fibre reinforced polymers including fibre Bragg grating sensors. *Composite Structures*. Online. 1 November 2022. Vol. 299, p. 116027. [Accessed 3 May 2023]. DOI 10.1016/J.COMPSTRUCT.2022.116027.
6. SHAFIGHFARD, Torkan and MIELOSZYK, Magdalena. Model of the Temperature Influence on Additively Manufactured Carbon Fibre Reinforced Polymer Samples with Embedded Fibre Bragg Grating Sensors. *Materials 2022, Vol. 15, Page 222*. Online. 28 December 2021. Vol. 15, no. 1, p. 222. [Accessed 5 May 2023]. DOI 10.3390/MA15010222.
7. LIU, Guang, XIONG, Yi and ZHOU, Limin. Additive manufacturing of continuous fiber reinforced polymer composites: Design opportunities and novel applications. *Composites Communications*. Online. 1 October 2021. Vol. 27, p. 100907. [Accessed 3 May 2023]. DOI 10.1016/J.COCO.2021.100907.
8. EDWIN RAJA DHAS, J. *Fiber-Reinforced Polymers Processes and Applications*. Online. New York : Nova Science Publishers, 2021. [Accessed 5 May 2023]. Available from: https://www.researchgate.net/publication/349426794
9. LUAN, Congcong, YAO, Xinhua, LIU, Chengzhe, LAN, Liujian and FU, Jianzhong. Self-monitoring continuous carbon fiber reinforced thermoplastic based on dual-material three-dimensional printing integration process. *Carbon*. 1 December 2018. Vol. 140, p. 100–111. DOI 10.1016/J.CARBON.2018.08.019.
10. ADIL, Samia and LAZOGLU, Ismail. A review on additive manufacturing of carbon fiber-reinforced polymers: Current methods, materials, mechanical properties, applications and challenges. *Journal of Applied Polymer Science*. Online. 15 February 2023. Vol. 140, no. 7, p. e53476. [Accessed 20 May 2023]. DOI 10.1002/APP.53476.
11. SEZER, H. Kürşad and EREN, Oğulcan. FDM 3D printing of MWCNT re-inforced ABS nano-composite parts with enhanced mechanical and electrical properties. *Journal of Manufacturing Processes*. 1 January 2019. Vol. 37, p. 339–347. DOI 10.1016/J.JMAPRO.2018.12.004.
12. LIU, Weihao, HUANG, Haihong, ZHU, Libin and LIU, Zhifeng. Integrating carbon fiber reclamation and additive manufacturing for recycling CFRP waste. *Composites Part B: Engineering*. Online. 15 June 2021. Vol. 215, p. 108808. [Accessed 19 May 2023]. DOI 10.1016/J.COMPOSITESB.2021.108808.

13. TIAN, Xiaoyong, LIU, Tengfei, WANG, Qingrui, DILMURAT, Abliz, LI, Dichen and ZIEGMANN, Gerhard. Recycling and remanufacturing of 3D printed continuous carbon fiber reinforced PLA composites. *Journal of Cleaner Production*. 20 January 2017. Vol. 142, p. 1609–1618. DOI 10.1016/J.JCLEPRO.2016.11.139.
14. CAROLO LUCAS, O'CONNELL JACKSON and PARENTI MATTEO. The Best Carbon Fiber Filaments of 2023 | All3DP. Online. 23 April 2023. [Accessed 20 May 2023]. Available from: https://all3dp.com/2/carbon-fiber-filament-explained-and-compared/
15. TODOROKI, Akira, OASADA, Tastuki, MIZUTANI, Yoshihiro, SUZUKI, Yoshiro, UEDA, Masahito, MATSUZAKI, Ryosuke and HIRANO, Yoshiyasu. Tensile property evaluations of 3D printed continuous carbon fiber reinforced thermoplastic composites. *Advanced Composite Materials*. Online. 3 March 2020. Vol. 29, no. 2, p. 147–162. [Accessed 3 January 2022]. DOI 10.1080/09243046.2019.1650323.
16. LUAN, Congcong, YAO, Xinhua, SHEN, Hongyao and FU, Jianzhong. Self-sensing of position-related loads in continuous carbon fibers-embedded 3D-printed polymer structures using electrical resistance measurement. *Sensors (Switzerland)*. Online. 1 April 2018. Vol. 18, no. 4. [Accessed 3 January 2022]. DOI 10.3390/s18040994.
17. IIZUKA, Keisuke and TODOROKI, Akira. Nonlinear behavior mechanism of change in electrical resistance on 3D printed carbon fiber / PA6 composites during cyclic tests. *Advanced Composite Materials*. 2022. DOI 10.1080/09243046.2022.2055514.
18. YE, Wenli, WU, Wenzheng, HU, Xue, LIN, Guoqiang, GUO, Jinyu, QU, Han and ZHAO, Ji. 3D printing of carbon nanotubes reinforced thermoplastic polyimide composites with controllable mechanical and electrical performance. *Composites Science and Technology*. 29 September 2019. Vol. 182. DOI 10.1016/J.COMPSCITECH.2019.05.028.
19. ZHENG, Si Xue, LUO, Xue Mei, WANG, Dong and ZHANG, Guang Ping. A novel evaluation strategy for fatigue reliability of flexible nanoscale films. *Materials Research Express*. Online. 7 March 2018. Vol. 5, no. 3, p. 035012. [Accessed 7 May 2023]. DOI 10.1088/2053-1591/AAB1C5.
20. HEIDARI-RARANI, M., RAFIEE-AFARANI, M. and ZAHEDI, A. M. Mechanical characterization of FDM 3D printing of continuous carbon fiber reinforced PLA composites. *Composites Part B: Engineering*. Online. 15 October 2019. Vol. 175. [Accessed 30 April 2023]. DOI 10.1016/J.COMPOSITESB.2019.107147.
21. GHIMIRE, Ritesh and LIOU, Frank. Coupled flexural-electrical evaluation of additively manufactured multifunctional composites at ambient temperature. *Applied Sciences (Switzerland)*. 1 October 2021. Vol. 11, no. 20. DOI 10.3390/APP11209638.
22. KALASHNYK, Nataliya, FAULQUES, Eric, SCHJØDT-THOMSEN, Jan, JENSEN, Lars R., RAUHE, Jens Chr M. and PYRZ, Ryszard. Monitoring self-sensing damage of multiple carbon fiber composites using piezoresistivity. *Synthetic Metals*. Online. 1 February 2017. Vol. 224, p. 56–62. [Accessed 13 April 2023]. DOI 10.1016/J.SYNTHMET.2016.12.021.
23. SHIRATORI, Hirohide, TODOROKI, Akira, UEDA, Masahito, MATSUZAKI, Ryosuke and HIRANO, Yoshiyasu. Compressive strength degradation of the curved sections of 3D-printed continuous carbon fiber composite. *Composites Part A: Applied Science and Manufacturing*. Online. 1 March 2021. Vol. 142. [Accessed 16 April 2023]. DOI 10.1016/J.COMPOSITESA.2020.106244.
24. RIMAŠAUSKAS, Marius, KUNCIUS, Tomas and RIMAŠAUSKIENĖ, Rūta. Processing of carbon fiber for 3D printed continuous composite structures. *Materials and Manufacturing*

Processes. Online. 3 October 2019. Vol. 34, no. 13, p. 1528–1536. [Accessed 5 May 2023]. DOI 10.1080/10426914.2019.1655152.
25. YAMAWAKI, Masao and KOUNO, Yousuke. Fabrication and mechanical characterization of continuous carbon fiber-reinforced thermoplastic using a preform by three-dimensional printing and via hot-press molding. *Advanced Composite Materials*. 4 March 2018. Vol. 27, no. 2, p. 209–219. DOI 10.1080/09243046.2017.1368840.
26. ANODAS. DC 12V KK-P40/20 30KG Electro Holding Magnet. Online. [Accessed 31 March 2023]. Available from: https://www.anodas.lt/elektromagnetas-12v-4-8w-30kg
27. RIGOL. *DG1000Z Series Function/Arbitrary Waveform Generator* Online. [no date]. [Accessed 31 March 2023]. Available from: https://www.batronix.com/pdf/Rigol/Datasheet/DG1000Z_DataSheet_EN.pdf
28. MMF. LV 102 manual. Online. [Accessed 31 March 2023]. Available from: https://www.mmf.de/manual/archiv/lv102man.pdf
29. FLUKE. *Technical Data* Online. [no date]. [Accessed 31 March 2023]. Available from: http://www.fluke.com
30. KEITHLEY. *2614B SMU technical specification* Online. [no date]. [Accessed 31 March 2023]. Available from: www.keithley.com
31. MEMMERT. *Product specification* Online. [no date]. [Accessed 31 March 2023]. Available from: https://www.pkpiran.com/wp-content/uploads/2021/04/UNB400-memmert-min.pdf
32. MEENA H. M., SINGH RANJAY and SANTRA PRIYABRATA. Design and Development of a Load-Cell Based Cost Effective Mini- Lysimeter. *Journal of Agricultural Physics*. Online. 2016. [Accessed 8 May 2023]. Available from: https://www.researchgate.net/publication/304784959_Design_and_Development_of_a_Load-Cell_Based_Cost_Effective_Mini-_Lysimeter
33. MANOALGA. Salary of mechanical engineers in Lithuania. Online. [Accessed 8 May 2023]. Available from: https://www.manoalga.lt/atlyginimu-informacija/mechanikos-inzinerija
34. MARKESTRO. Markestro electricity price. Online. [Accessed 8 May 2023]. Available from: https://markestro.lt/elektra/elektros-kainos-ir-tarifai
35. LEMONA. PLA filament retail prices . Online. [Accessed 8 May 2023]. Available from: https://www.lemona.lt/robotika-ir-atvirojo-kodo-elektronika/3d-spausdinimas/plastikas-3d-spausdinimui?page=1&ep_string_2247=PLA
36. EASY COMPOSITES. Carbon fiber strand price. Online. [Accessed 8 May 2023]. Available from: https://www.easycomposites.co.uk/3k-carbon-fibre-tow
37. CLEVER CREATIONS. FDM 3D printer power consumption. Online. [Accessed 8 May 2023]. Available from: https://clevercreations.org/how-much-electricity-3d-printer-power-usage/

Appendices

Appendix 1. Program code used to measure resistance periodically

```
-- Restore 2600B defaults.
smua.reset()
-- Select measure I autorange.
smua.measure.autorangei = smua.AUTORANGE_ON
-- Select measure V autorange.
smua.measure.autorangev = smua.AUTORANGE_ON
-- Select ASCII data format.
format.data = format.ASCII
-- Set the buffer count to 7200.
smua.measure.count = 7200
-- Set the measure interval to 0.05 s.
smua.measure.interval = 0.05
-- Select the source voltage function.
smua.source.func = smua.OUTPUT_DCVOLTS
-- Set the source voltage to output 1 V.
smua.source.levelv = 1
-- Turn on the output.
smua.source.output = smua.OUTPUT_ON
-- Create a temporary reading buffer.
mybuffer = smua.makebuffer(smua.measure.count)
-- Store current readings in mybuffer.
smua.measure.overlappedr(mybuffer)
-- Wait for the buffer to fill.
waitcomplete()
-- Turn off the output.
smua.source.output = smua.OUTPUT_OFF
-- Output readings 1 to 100 from mybuffer.
printbuffer(1, 100, mybuffer)
-- Delete mybuffer.
--mybuffer = nil
--smua.savebuffer(mybuffer,"csv", "mybuffer.csv")
smua.savebuffer(smua.mybuffer,"csv","/usb1/mybuffer.csv")
-- Delete mybuffer.
mybuffer = nil
```